
(NASA-TM-X-72684) EFFECTS OF LANDING GEAR, SPEED BRAKE AND PROTUBERANCES ON THE LONGITUDINAL AERODYNAMIC CHARACTERISTICS OF AN NASA SUPERCRITICAL-WING RESEARCH AIRPLANE MODEL (NASA) 55 p HC A04/MF A01 CSCL 01A G3/02

N83-11085

Unclas 32201

~~CONFIDENTIAL~~

NASA TECHNICAL MEMORANDUM

NASA TM X-72684

COPY NO.

NASA TM X-72684

EFFECTS OF LANDING GEAR, SPEED BRAKE AND PROTUBERANCES ON THE LONGITUDINAL AERODYNAMIC CHARACTERISTICS OF AN NASA SUPERCRITICAL WING RESEARCH AIRPLANE MODEL

By Dennis W. Bartlett and Giuliana Sangiorgio

[redacted]

[redacted]

NATIONAL AERONAUTICS AND SPACE ADMINISTRATION
LANGLEY RESEARCH CENTER, HAMPTON, VIRGINIA 23665

~~CONFIDENTIAL~~

[redacted]

[redacted]

1. Report No.	2. Government Accession No.	3. Recipient's Catalog No.
TM X-72684		

4. Title and Subtitle: Effects of Landing Gear, Speed Brake and Protuberances on the Longitudinal Aerodynamic Characteristics of an NASA Supercritical-Wing Research Airplane Model [redacted]

5. Report Date: July 1975

6. Performing Organization Code

7. Author(s): Dennis W. Bartlett and Giuliana Sangiorgio

8. Performing Organization Report No.

9. Performing Organization Name and Address

NASA Langley Research Center
Hampton, VA 23665

10. Work Unit No.: 505-11-11-04

11. Contract or Grant No.

Technical Memorandum

12. Sponsoring Agency Name and Address

National Aeronautics & Space Administration
Washington, DC 20546

13. Type of Report and Period Covered: Technical Memorandum

14. Sponsoring Agency Code

15. Supplementary Notes

Special technical information release, not planned for formal NASA publication.

16. Abstract

An investigation has been conducted in the Langley Research Center 8-foot transonic pressure tunnel to determine the effects of the landing gear, speed brake and the major airplane protuberances on the longitudinal aerodynamic characteristics of an 0.087-scale model of the TF-8A supercritical-wing research airplane. For the effects of the landing gear and speed brake, tests were conducted at Mach numbers of 0.25 and 0.35 with a flap deflection of 20° and a horizontal-tail angle of -10°. These conditions would simulate those required for take-off and landing. The effects of the protuberances were determined with the model configured for cruise (i.e., horizontal-tail angle of -2.5° and no other control deflection), and these tests were conducted at Mach numbers from 0.50 to 1.00. The angle-of-attack range for all tests varied from about -5° to 12°.

ORIGINAL PAGE IS OF POOR QUALITY

ORIGINAL PAGE IS OF POOR QUALITY

17. Key Words (Suggested by Author(s))

TF-8A supercritical wing research airplane
Landing gear
Protuberances

18. Distribution Statement

[redacted]

19. Security Classif. (of this report)	20. Security Classif. (of this page)	21. No. of Pages	22. Price
[redacted]	Unclassified		

[redacted]

1981

~~CONFIDENTIAL~~

~~CONFIDENTIAL~~

EFFECTS OF LANDING GEAR, SPEED BRAKE AND PROTUBERANCES ON THE LONGITUDINAL AERODYNAMIC CHARACTERISTICS OF AN NASA SUPERCRITICAL-WING RESEARCH AIRPLANE MODEL

By Dennis W. Bartlett and Giuliana Sangiorgio

Langley Research Center

SUMMARY

An investigation has been conducted in the Langley Research Center 8-foot transonic pressure tunnel to determine the effects of the landing gear, speed brake and the major airplane protuberances on the longitudinal aerodynamic characteristics of an 0.087-scale model of the TF-8A supercritical-wing research airplane. For the effects of the landing gear and speed brake, tests were conducted at Mach numbers of 0.25 and 0.35 with a flap deflection of 20° and a horizontal-tail angle of -10°. These conditions would simulate those required for take-off and landing. The effects of the protuberances were determined with the model configured for cruise (i.e. horizontal-tail angle of -2.5° and no other control deflection), and these tests were conducted at Mach numbers from 0.50 to 1.00. The angle-of-attack range for all tests varied from about -5° to 12°.

The extension of the landing gear resulted in a slight increase in lift and a small negative shift in pitching moment (less than a comparable change in horizontal-tail angle of 0.5°) throughout the angle-of-attack range of the investigation. The deployment of the speed brake (deflected 15°), however, showed no appreciable effects on either the lift or pitching-moment characteristics. As would be expected, the landing gear and speed brake did cause a significant

~~CONFIDENTIAL~~

increase in drag, however, this increase was substantially larger near the minimum drag point ($\alpha \approx 1°$) than at the take-off and landing angle of attack of 8.5°.

The effect of the protuberances on the lift and pitching-moment characteristics is negligible, however, there is a small increase in drag throughout most of the lift-coefficient range at all Mach numbers. At the cruise lift coefficient of 0.4, the drag increment due to protuberances varies from about 0.0003 in drag coefficient at a Mach number of 0.50 to approximately 0.0008 at 0.95 Mach number. However, at the wing design Mach number of 0.99, the drag increment near 0.4 lift coefficient is about 0.0002 in drag coefficient.

INTRODUCTION

In support of the flight-test program and simulator studies for the TF-8A supercritical-wing research airplane (ref. 1) and to establish the necessary data base for a correlation of wind-tunnel and flight data, extensive wind-tunnel tests have been conducted involving this airplane. In addition to configuration development-type programs (see refs. 2, 3, and 4 for example.), investigations were performed to determine the basic longitudinal and lateral static stability characteristics (ref. 5), the dynamic stability characteristics (ref. 6) and wing and fuselage pressure distributions (refs. 7 and 8). The purpose of this paper is to document the results of wind-tunnel tests that were conducted to determine the effects of the landing gear and speed brake on the longitudinal aerodynamic characteristics of the TF-8A supercritical-wing research airplane at Mach numbers near those for take-off and landing (M = 0.25 and 0.35). In addition, the effects of the major airplane protuberances (i.e. antennae, nose probe, etc.) on the longitudinal aerodynamic characteristics are presented at Mach numbers from 0.50 to 1.00. Tests were conducted over an angle-of-attack range that varied from about -5° to about 12° and at Reynolds numbers which varied from approximately 10.2×10^{6} per m (3.1×10^{6} per ft) at 0.25 Mach number to a maximum of about 20.0×10^{6} per m (6.1×10^{6} per ft) at 0.80 Mach number. Near Mach 1.0, the test Reynolds number was about 16.0×10^{6} per m (4.9×10^{6} per ft).

SYMBOLS

The longitudinal aerodynamic characteristics presented herein are referred to the stability axis system. Force and moment data have been reduced to conventional coefficient form based on the geometry of the reference wing planform, which is the planform produced by extending the straight leading and trailing edges of the outboard sections of the wing to the fuselage center line. (See fig. 1(a).) Moments are referenced to the quarter-chord point (fuselage station 99.45 cm (39.155 in.)) of the mean geometric chord of the reference wing panel. All dimensional values are given in both SI and U.S. Customary Units; however, measurements and calculations were made in U.S. Customary Units.

Coefficients and symbols used herein are defined as follows:

b wing span, 114.30 centimeters (45.00 inches)

C_D drag coefficient, $\frac{\text{Drag}}{qS}$

C_L lift coefficient, $\frac{\text{Lift}}{qS}$

C_m pitching-moment coefficient, $\frac{\text{Pitching moment}}{qS\bar{c}}$

$\bar{c}$ mean geometric chord of reference wing panel, 18.09 centimeters (7.121 inches)

c local streamwise chord of wing

M free-stream Mach number

q free-stream dynamic pressure

S area of reference wing planform including fuselage intercept, 0.193 meter^2 (2.075 feet^2)

α angle of attack, referred to a model water line, degrees

δ_h horizontal tail deflection angle, referred to model water line (positive when trailing edge is down), degrees

δ_f flap deflection angle (positive when trailing edge is down), degrees

TEST FACILITY

The investigation was conducted in the Langley Research Center 8-foot transonic pressure tunnel (ref. 9). This facility is a continuous-flow, single-return, rectangular slotted-throat tunnel having controls that allow for the independent variation of Mach number, density, stagnation temperature and dew-point. The test section is square in cross section with the upper and lower walls axially slotted (each wall having an open ratio of approximately 0.06) to permit changing the test-section Mach number continuously through the transonic speed range. The stagnation pressure in the tunnel can be varied from a minimum value of about 0.25 atmosphere at all test Mach numbers to a maximum value of approximately 1.5 atmospheres at transonic Mach numbers and approximately 2.0 atmospheres at Mach numbers of 0.40 or less.

MODEL DESCRIPTION

Geometric characteristics of the 0.087-scale research airplane model are presented in figure 1, and photographs of the model are presented as figure 2. The basic fuselage and tails are scaled versions of those utilized on the test-bed airplane (TF-8A). The model was equipped with flow-through ducts which discharge at the base of the fuselage on either side of the flat-sided model support sting. Internal drag coefficients and mass-flow ratios are contained in ref. 5.

The wing used during the investigation to determine the effects of the landing gear and speed brake was constructed of aluminum. A flap deflection of 20° was employed for these tests with a horizontal-tail angle of -10°. These flap and tail angles are those that were estimated to be required for take-off and landing. Flap and aileron control-effectiveness data obtained with this aluminum "control" wing are contained in references 10 and 11. To obtain wind-tunnel performance and pressure data for the research airplane, a separate steel wing was normally employed (see ref. 2 for example), and it was the steel wing that was used during the present tests to determine the effects of the major airplane protuberances. Both wings are geometrically the same, and coordinates are presented in reference 2.

The supercritical wing was mounted on the fuselage at a root-chord incidence angle of 1.5° and has approximately 5° of twist (washout) from root to tip in the unloaded condition. The reference wing planform, which excludes the leading-edge glove and trailing-edge extension, has a taper ratio of 0.36, an aspect ratio of 6.8, and 42.24° of sweepback at the quarter-chord line. The area of the reference wing planform including the fuselage intercept is 0.193 m^2 (2.075 ft^2), and the mean geometric chord of the reference wing panel is 18.09 cm (7.121 in.).

Details of the model landing gear and speed brake are presented in figures 1(b), 1(c) and 1(d), and the landing gear and speed brake are shown on the model in the photographs of figure 2. The basic aircraft speed brake, deflected approximately 15°, was used during landing to aid in stopping the airplane which was not provided with a drogue chute. Details of the major airplane protuberances are presented in figure 1(e), and these protuberances are also shown in the photographs of figure 2.

The underwing, leading-edge vortex generators (fig. 1(f)) were employed on both model wings (60-percent-wing-semispan station) for all tests of the present investigation, however, the aileron hinge fairings (fig. 1(g) and 1(h)) were included only on the steel wing. The underwing, leading-edge vortex generators are discussed in references 3 and 12, and limited results for the effects of the aileron hinge fairings are also presented in reference 3.

MEASUREMENTS AND TEST CONDITIONS

Measurements of overall forces and moments on the model were obtained from a six-component, electrical strain-gage balance housed within the fuselage cavity. Differential pressure transducers referenced to free-stream static pressure were used to measure the pressure in the fuselage balance chamber and at the model base.

The effects of the landing gear and speed brake were measured at Mach numbers of 0.25 and 0.35 for a flap setting of 20° and a horizontal-tail angle of -10°. For determination of the protuberance effects, the model had no control deflection other than a horizontal-tail angle of -2.5° (estimated to be that required for trim at the design-cruise condition), and measurements were obtained at Mach numbers from 0.50 to 1.00. The angle-of-attack range for all tests varied from about -5° to approximately 12° for a sideslip angle of 0°. The tunnel test conditions at the Mach numbers of the present investigation are presented in table I.

Boundary-Layer Transition

The boundary-layer trip arrangements used for the wing are shown in figure 3. No. 120 Carborundum grains were located on the horizontal and vertical tails at 5 percent of the local streamwise chords and were also applied 2.54 cm (1.00 in.) aft of the model nose and 1.27 cm (0.50 in.)

rearward of the inlet lip on both the inner and outer surfaces. All boundary-layer trips were applied to the model in bands that were 0.127 cm (0.05 in.) wide and were located by measurements taken in the streamwise direction.

Corrections

Drag coefficients contained herein have been adjusted to correspond to a condition of free-stream static pressure acting in the balance chamber and at the model base (excluding the duct exit area). No adjustments have been made to the drag, however, for internal duct drag. (See ref. 5.)

Corrections have been made to the measured angles of attack to account for deflection of the model balance and sting support system under aerodynamic load and for tunnel airflow angularity.

PRESENTATION OF RESULTS

The results of this investigation are presented in the following figures:

DISCUSSION OF RESULTS

Effects of Landing Gear and Speed Brake

The effects of the landing gear and the speed brake on the longitudinal aerodynamic characteristics are presented in figure 4 at Mach numbers 0.25 and 0.35 (take-off and landing Mach number range). From this figure it can be seen that the extension of the landing gear causes a small increase in lift throughout the angle-of-attack range. This is probably due to the fact that the relatively large main gear doors (fig. 1(c)), which form an angle of about 20° with the horizontal in the deployed state, are producing lift. In addition, the deployment of the landing gear also results in a small negative shift in pitching moment ($\Delta C_m \approx 0.015$) throughout the majority of the angle-of-attack range, however, this only amounts to a comparable change in horizontal-tail angle of less than 0.5°. The speed brake (deflected ≈ 15°) has only negligible effects on the lift and the pitching-moment characteristics. (See fig. 4.)

Near minimum drag ($\alpha \approx 1°$), the landing gear causes an increase in drag of approximately 50 percent over the basic configuration, while the speed brake results in about a 23 percent drag increase. However, near the angle of attack for take-off and landing ($\alpha = 8.5°$), the drag increase resulting from the landing gear and speed brake is about 29 percent and 11 percent respectively. As would be expected, there is little variation in the effects noted above between the two Mach numbers at which data are presented in figure 4 ($M = 0.25$ and 0.35).

Effect of Protuberances

The term "protuberances", as used in this report, includes the airspeed probe, the camera fairing plate, the PCM antenna, the anticollision light and the drain valve (fig. 1(e)).

The effect of the protuberances on the longitudinal aerodynamic characteristics is presented in figure 5 at Mach numbers from 0.5 to 1.0, and the drag increment due to protuberances is presented in figure 6 at lift coefficients of 0.1 and 0.4.

The protuberances have no appreciable effect on the lift and pitching-moment characteristics, however, as would be expected, there is a small increase in drag throughout most of the lift-coefficient range at all Mach numbers presented in figure 5. At the cruise lift coefficient of 0.4, the protuberance drag increment varies from about 0.0003 in drag coefficient at a Mach number 0.50 to about 0.0006 at 0.95 Mach number. However, at the wing design Mach number of 0.99, the drag increment due to protuberances near 0.4 lift coefficient is about 0.0002 in drag coefficient (See fig. 6.) Similar effects are also noted in figure 6 at a lift coefficient of 0.1 which is near minimum drag.

The drag increments due to surface defects (slots, gaps, scratches, etc.) for the basic TF-8A airplane are documented in reference 13. These drag increments along with those reported herein must, of course, be considered when attempting to extrapolate wind-tunnel derived drag data to full-scale conditions. (See for example, paper 5 of ref. 1.)

~~CONFIDENTIAL~~

OF

REFERENCES

1. Anon: Supercritical Wing Technology - A Progress Report on Flight Evaluations. NASA SP-301, 1972.
2. Bartlett, Dennis W.; and Harris, Charles D.: Aerodynamic Characteristics of an NASA Supercritical-Wing Research Airplane Model With and Without Fuselage Area-Rule Additions at Mach 0.25 to 1.00. NASA TM X-2633, 1972.
3. Bartlett, Dennis W.; Harris, Charles D.; and Kelly, Thomas C.: Wind-Tunnel Development of Underwing Leading-Edge Vortex Generators on an NASA Supercritical-Wing Research Airplane Configuration. NASA TM X-2808, 1973.
4. Bartlett, Dennis W.; and Harris, Charles D.: Effects of Wing Trailing-Edge Truncation on the Aerodynamic Characteristics of an NASA Supercritical-Wing Research Airplane Model. NASA TM X-3024, 1974.
5. Bartlett, Dennis W.; and Re, Richard J.: Wind-Tunnel Investigation of Basic Aerodynamic Characteristics of a Supercritical-Wing Research Airplane Configuration. NASA TM X-2470, 1972.
6. Boyden, Richmond P.: Dynamic-Stability Characteristics in Pitch, Yaw, and Roll of a Supercritical Wing Research Airplane Model. NASA TM X-2900, 1974.
7. Harris, Charles D.: Wind-Tunnel Measurements of Aerodynamic Load Distribution on an NASA Supercritical-Wing Research Airplane Configuration. NASA TM X-2469, 1971.
8. Harris, Charles D.; and Bartlett, Dennis W.: Tabulated Pressure Measurements on an NASA Supercritical-Wing Research Airplane Model With and Without Fuselage Area-Rule Additions at Mach 0.25 to 1.00. NASA TM X-2634, 1972.

~~CONFIDENTIAL~~

9. Schaefer, William T., Jr.: Characteristics of Major Active Wind Tunnels at Langley Research Center. NASA TM X-1130, 1965.

10. Bartlett, Dennis W.: Effects of Differential and Symmetrical Aileron Deflection on the Longitudinal and Lateral Aerodynamic Characteristics of an NASA Supercritical-Wing Research Airplane Model. NASA TM X-3231, 1975.

11. Re, Richard J.: Stability and Control Characteristics, Including Aileron Hinge Moments, of a Model of a Supercritical-Wing Research Airplane. NASA TM X-2929, 1974.

12. Harris, Charles D.; and Bartlett, Dennis W.: Wind-Tunnel Investigation of Effects of Underwing Leading-Edge Vortex Generators on a Supercritical-Wing Research Airplane Configuration. NASA TM X-2471, 1972.

13. Horton, Elmer A.; and Tetervin, Neal: Measured Surface Defects on Typical Transonic Airplanes and Analysis of Their Drag Contributions. NASA TN D-1024, 1962.

TABLE I.- TUNNEL TEST CONDITIONS

Mach number	Temperature		Reynolds number	
	K	°F	per m	per ft
1.00	322	120	15.9×10^6	4.8×10^6
.99	322	120	16.1	4.9
.98	322	120	16.1	4.9
.97	322	120	16.1	4.9
.95	322	120	16.4	5.0
.90	322	120	18.4	5.6
.80	322	120	20.0	6.1
.50	322	120	14.4	4.4
.35	322	120	7.2	2.2
.25	322	120	10.2	3.1

~~CONFIDENTIAL~~

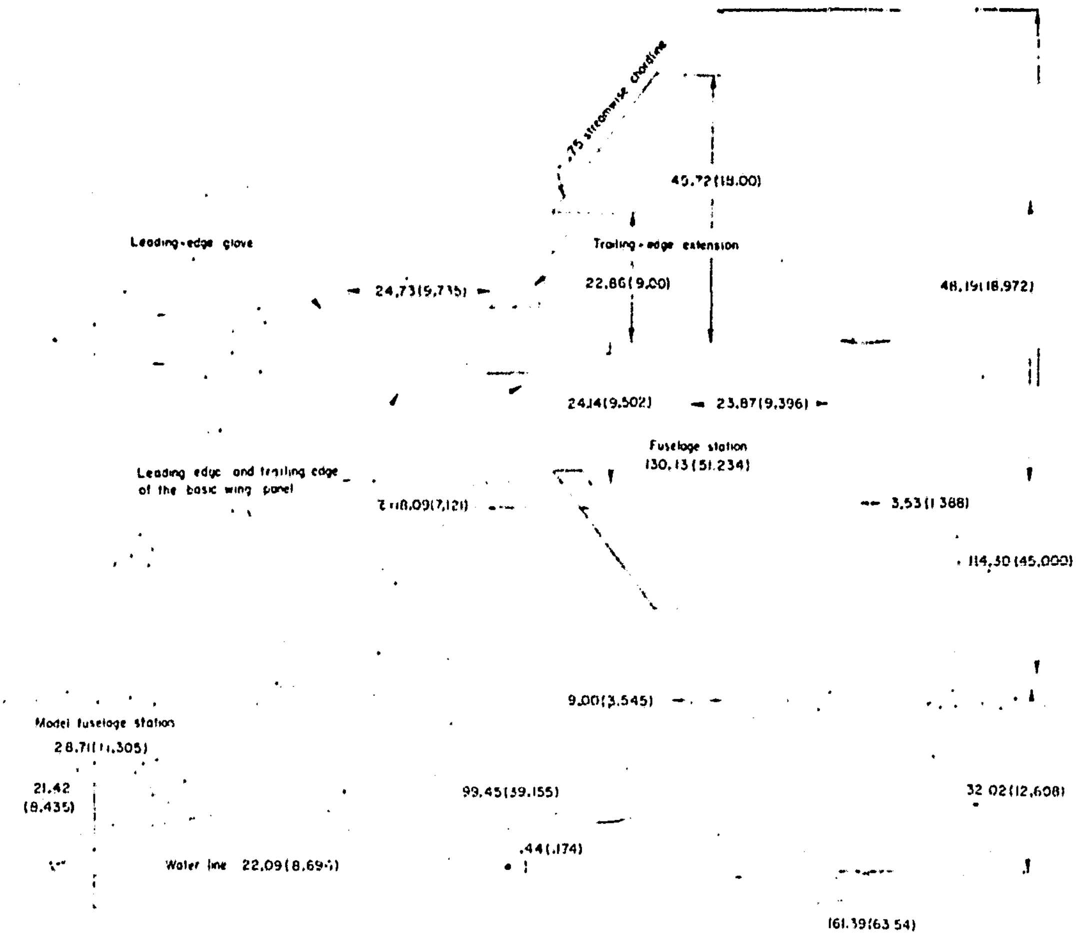

(a) General arrangement of 0.087-scale model.

Figure 1.- Model details. Dimensions are given in centimeters (inches).

~~CONFIDENTIAL~~

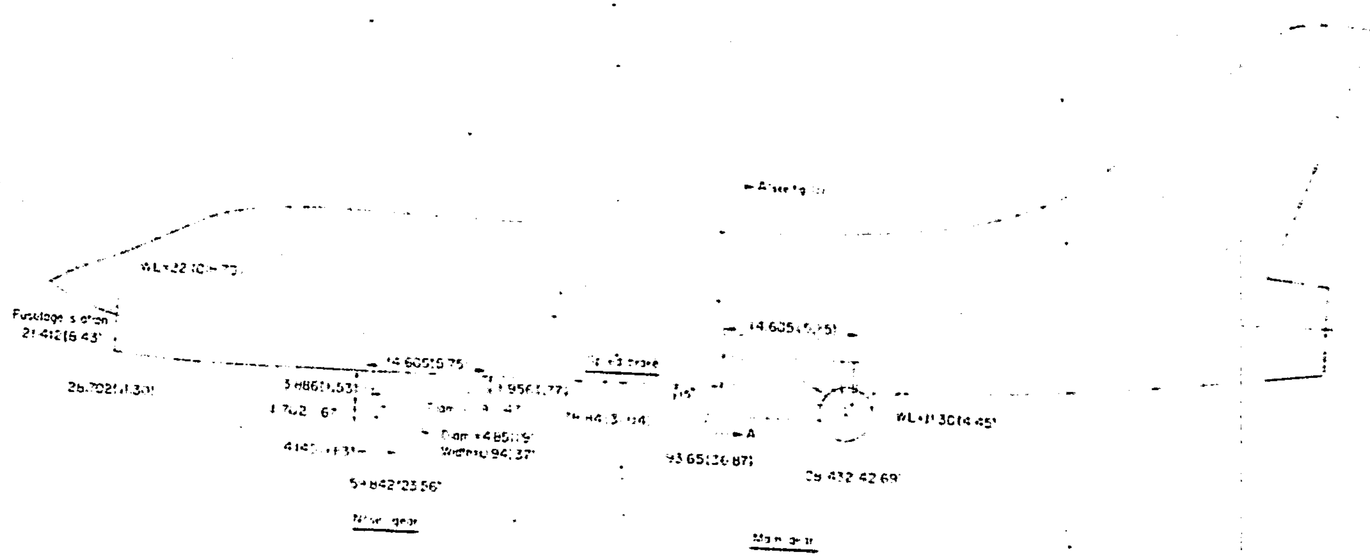

(b) Landing gear and speed brake arrangement.

Figure I. - Continued.

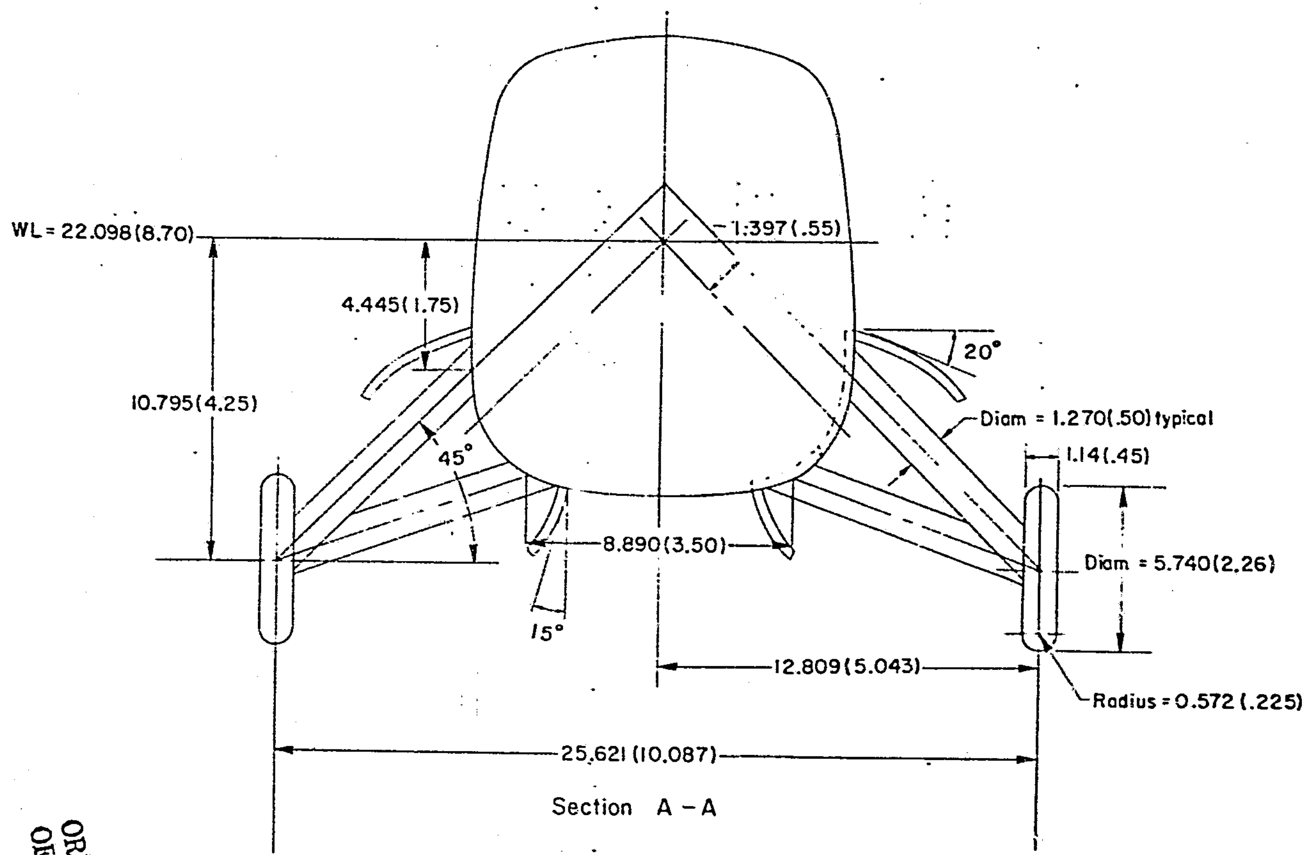

Section A – A

(c) Main gear arrangement.

Figure 1.- Continued.

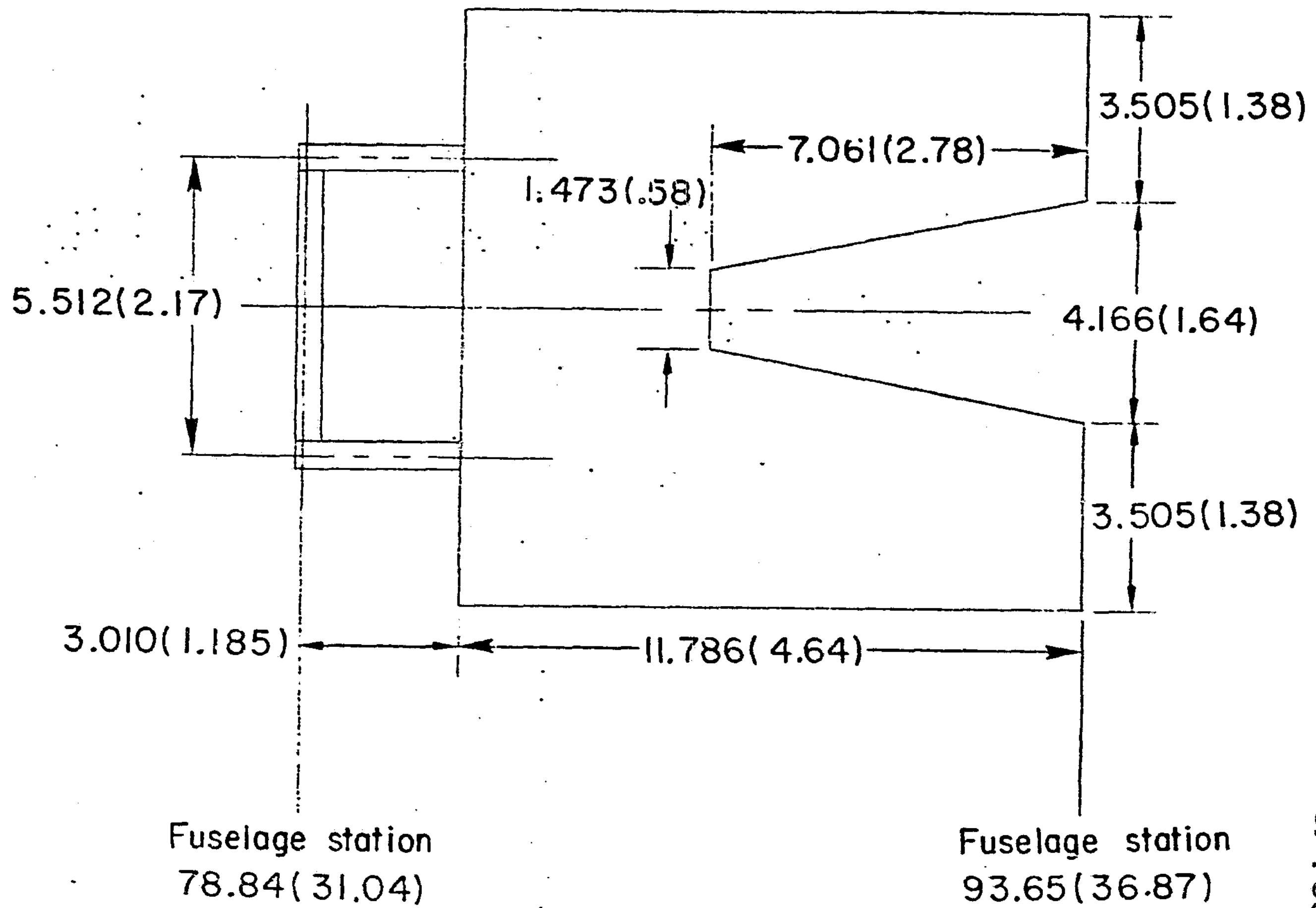

(d) Speed brake planform.

Figure 1.- Continued.

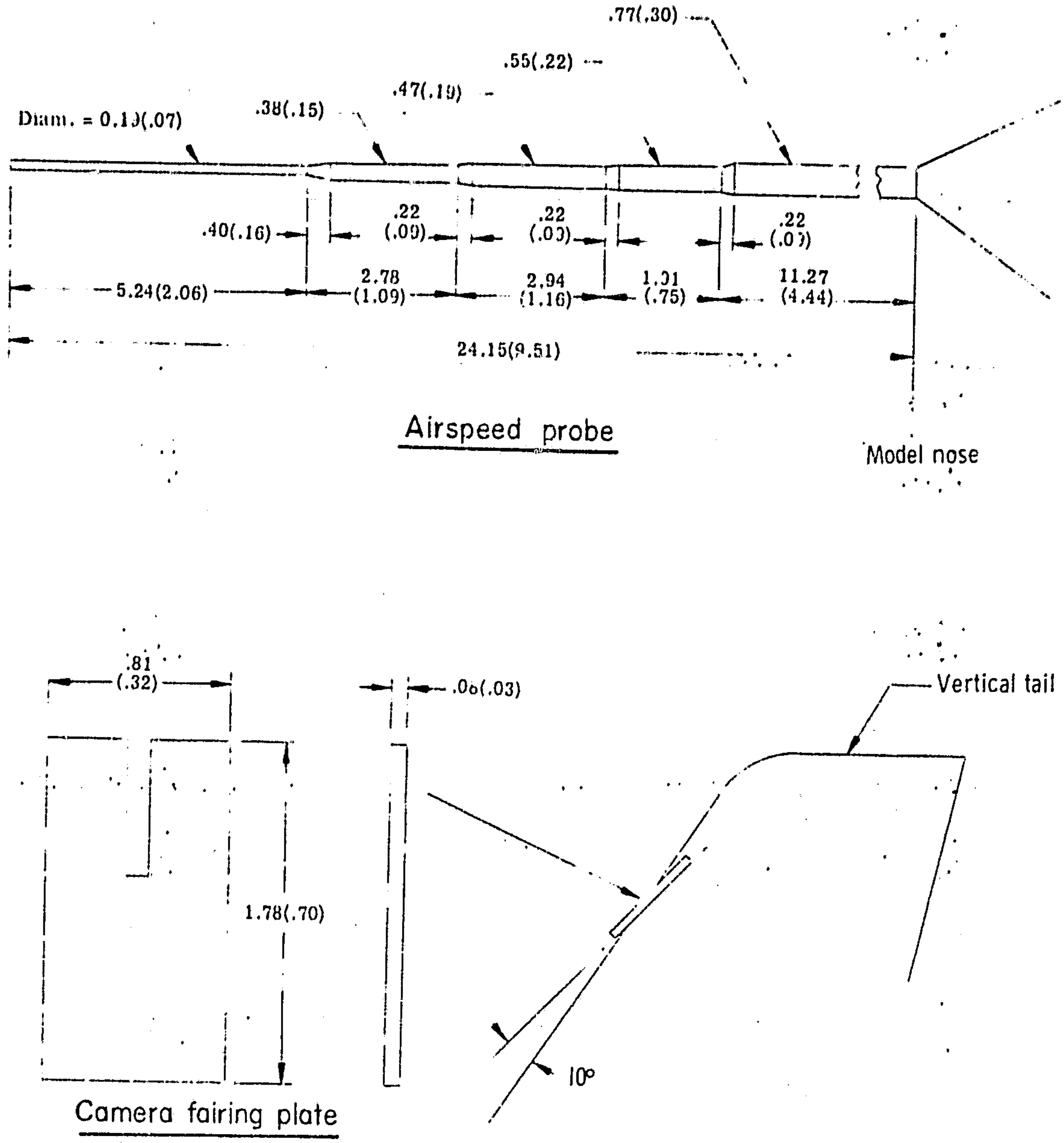

(e) Simulated full-scale airplane protuberances.

Figure 1.- Continued.

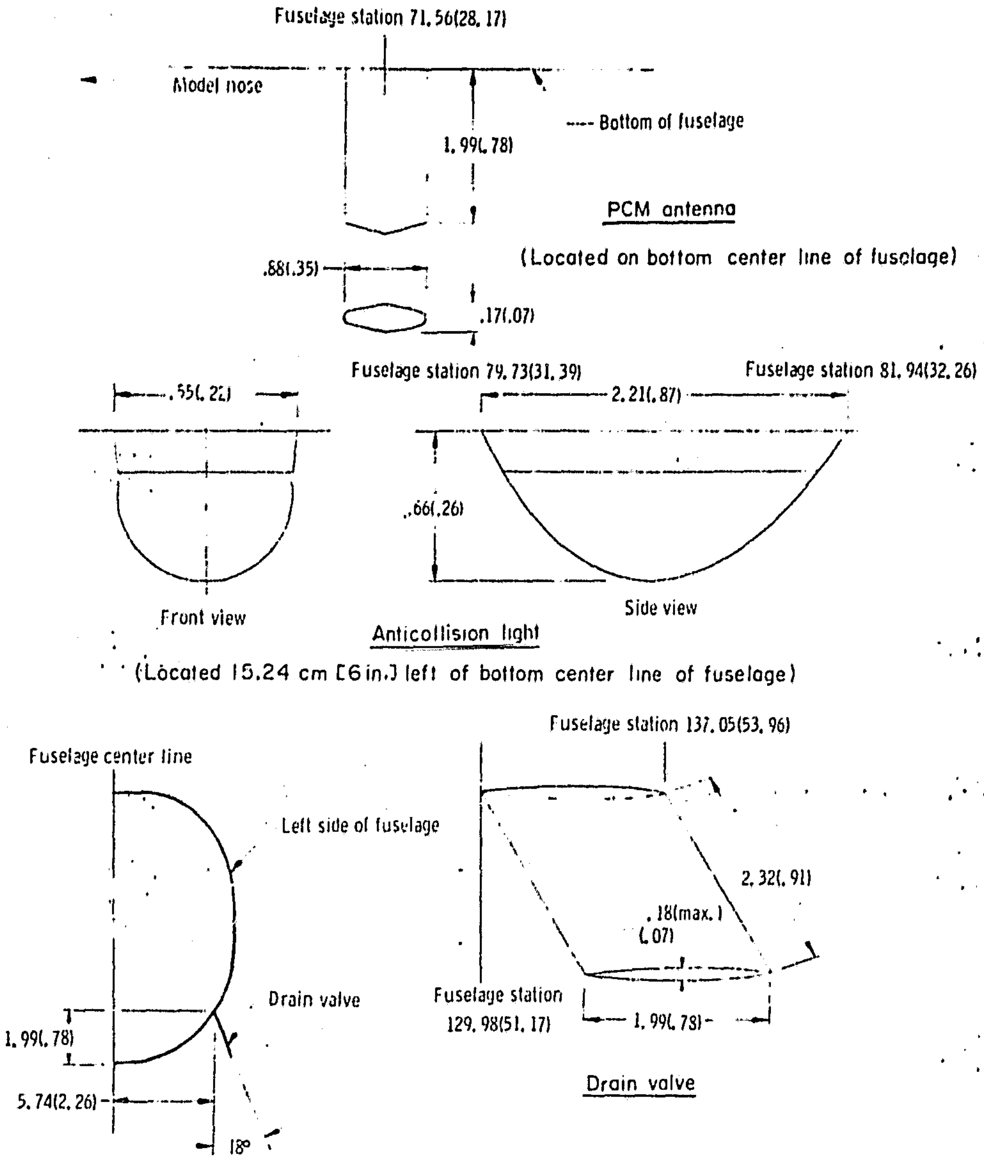

(e) Simulated full-scale airplane protuberances. Concluded.

Figure 1.- Continued.

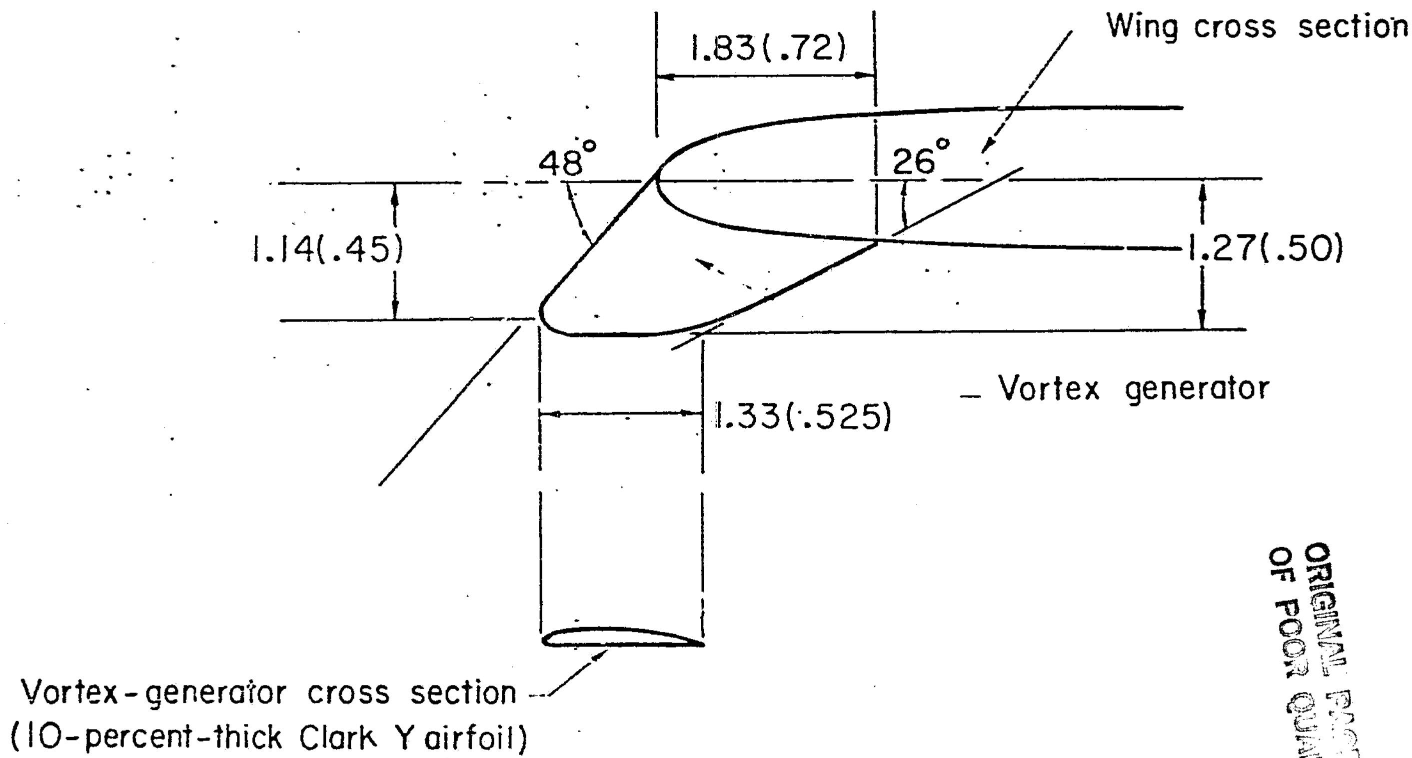

(f) Vortex generator.

Figure 1.- Continued.

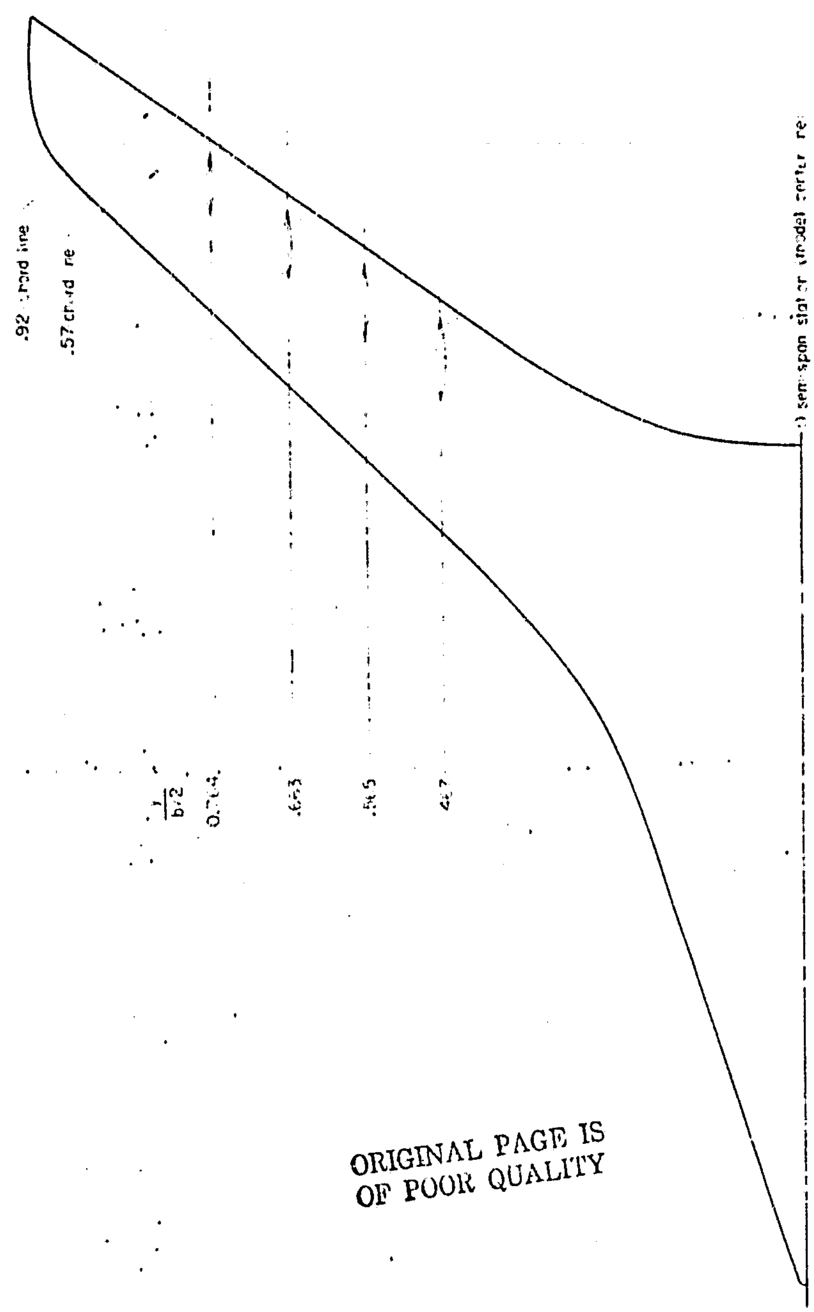

(g) Location of aileron hinge fairings.

Figure I.- Continued.

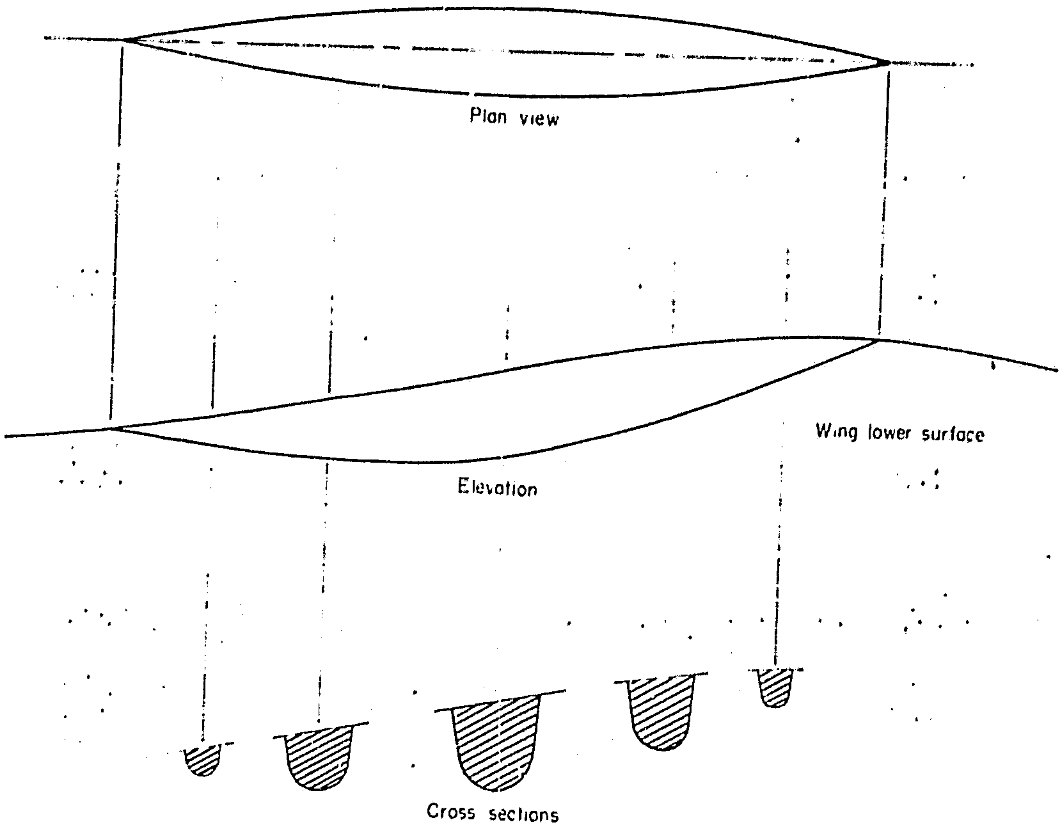

(h) Cross section of aileron hinge fairings.

Figure I.- Concluded.

~~CONFIDENTIAL~~

ORIGINAL PAGE IS
OF POOR QUALITY

[redacted]

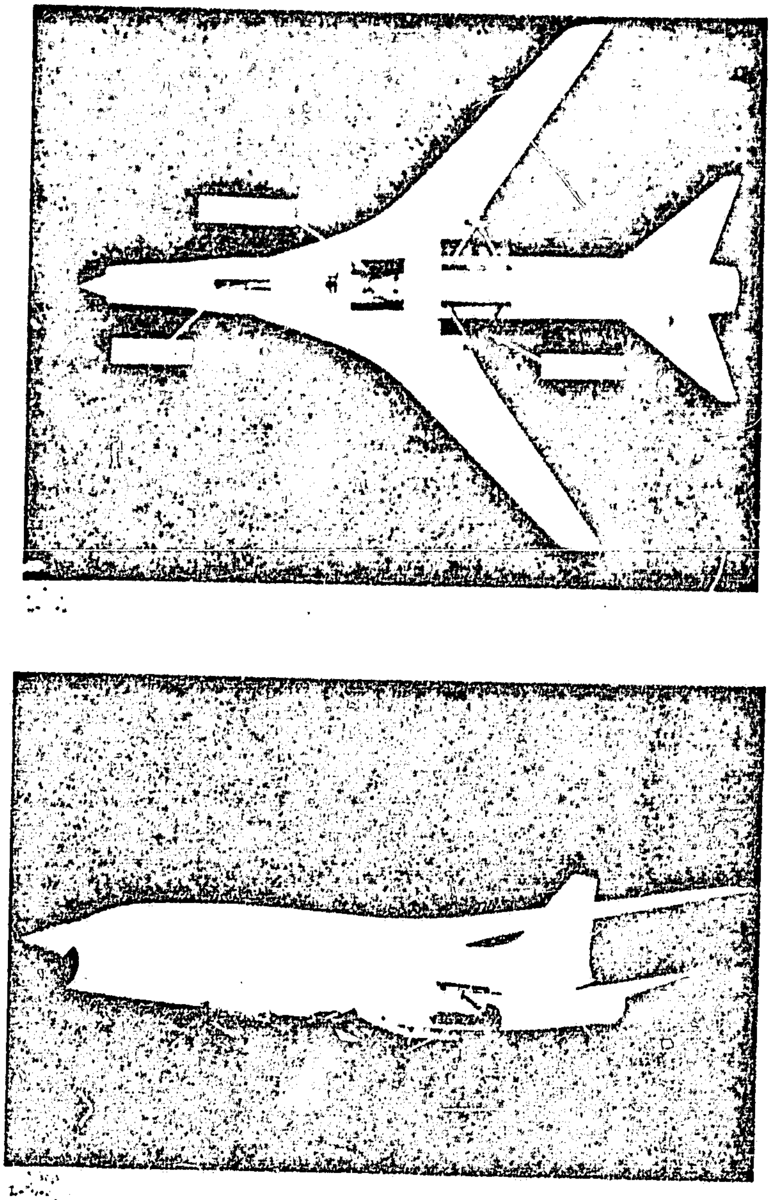

[redacted]

Figure 2. - Model photographs.

ORIGINAL PAGE IS
OF POOR QUALITY

~~CONFIDENTIAL~~

[redacted]

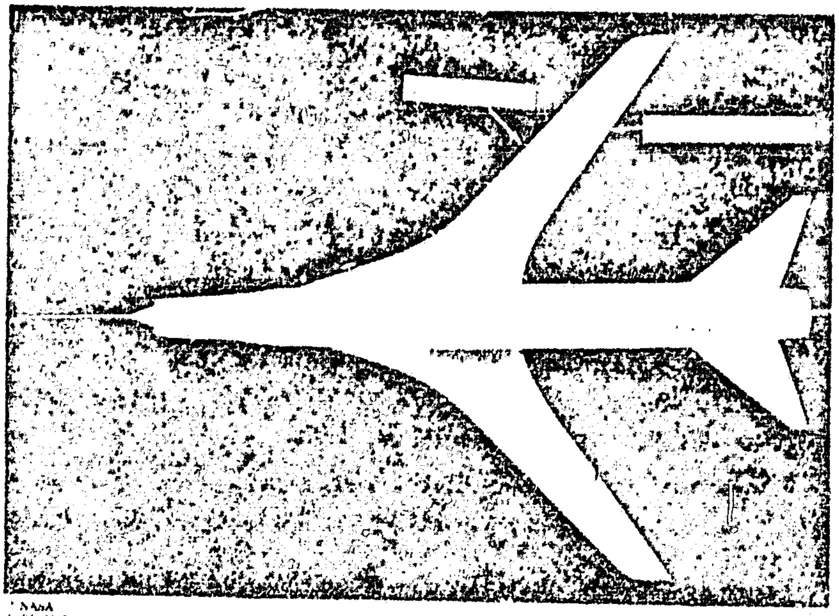

NASA

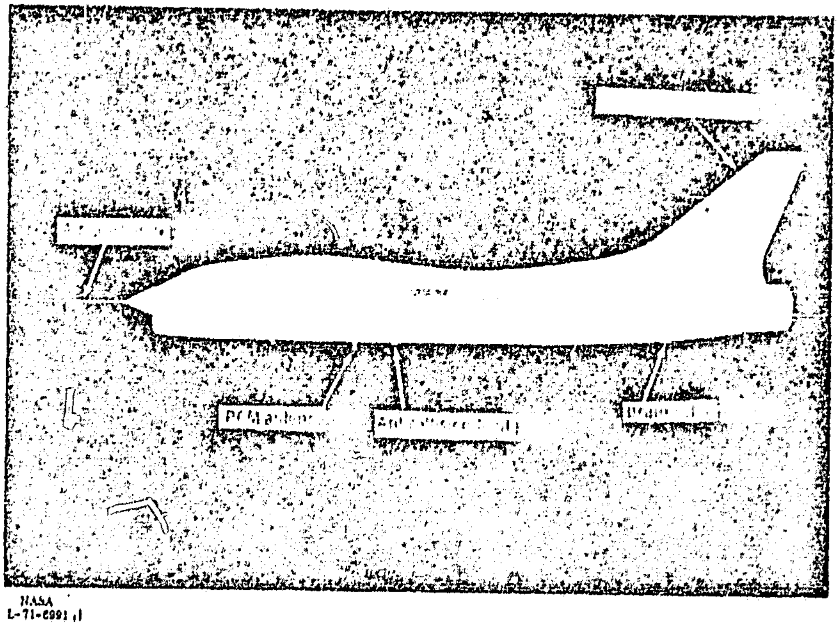

NASA
L-71-6991

Figure 2. - Concluded.

[redacted]

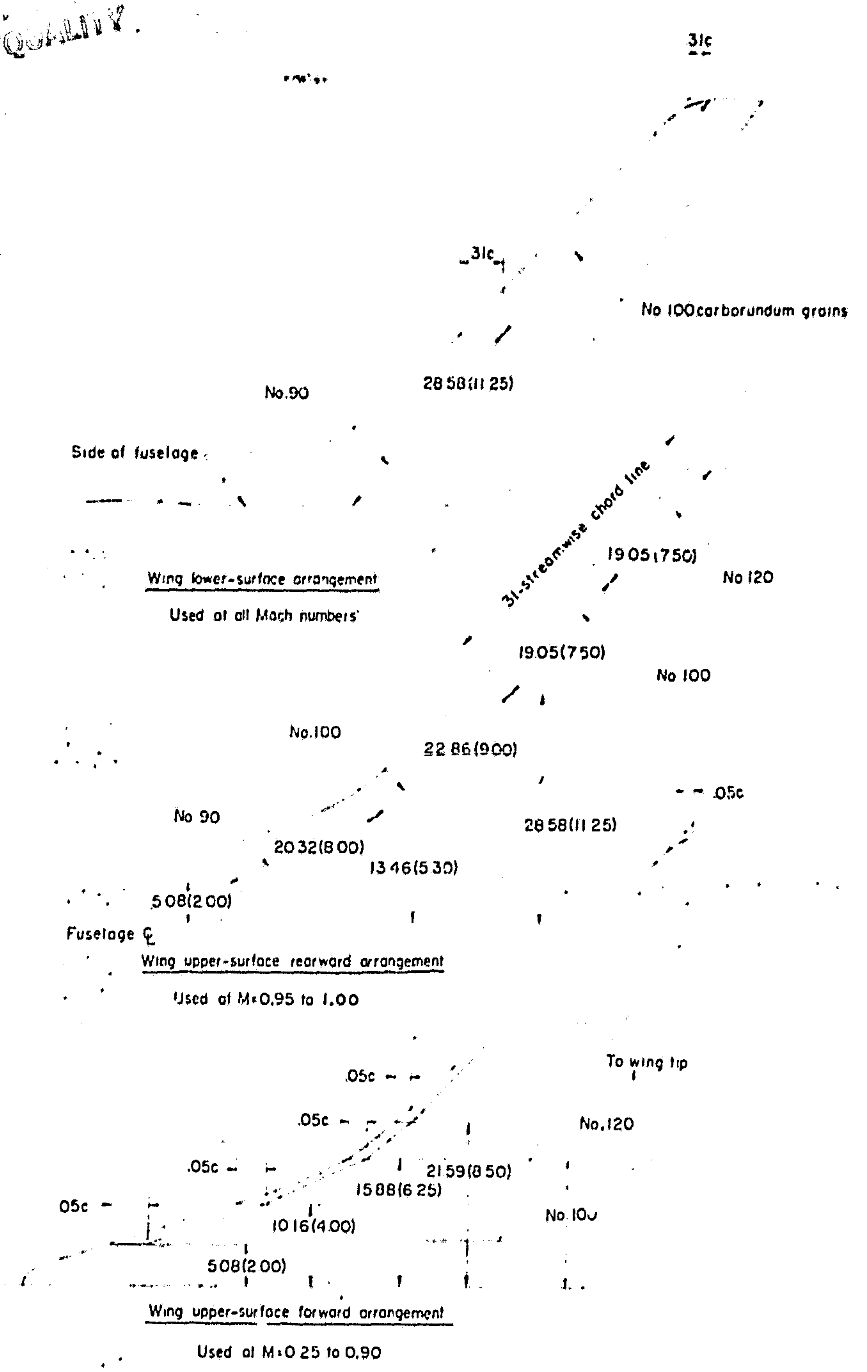

Figure 3.- Wing boundary-layer trip arrangements. Dimensions are in cm (in.).

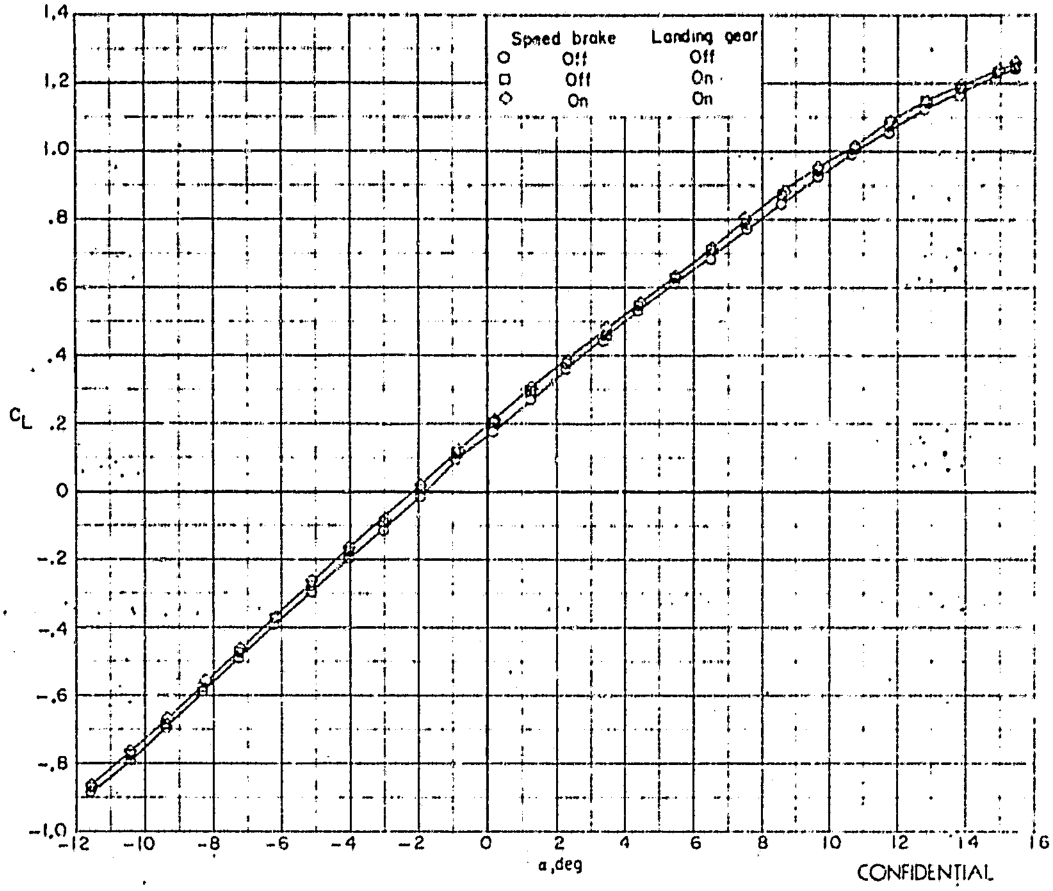

(a) M = 0.25.

Figure 4.- Effects of landing gear and speed brake on the longitudinal characteristics. $\delta_h = -10°$; $\delta_f = 20°$.

ORIGINAL PAGE IS OF POOR QUALITY

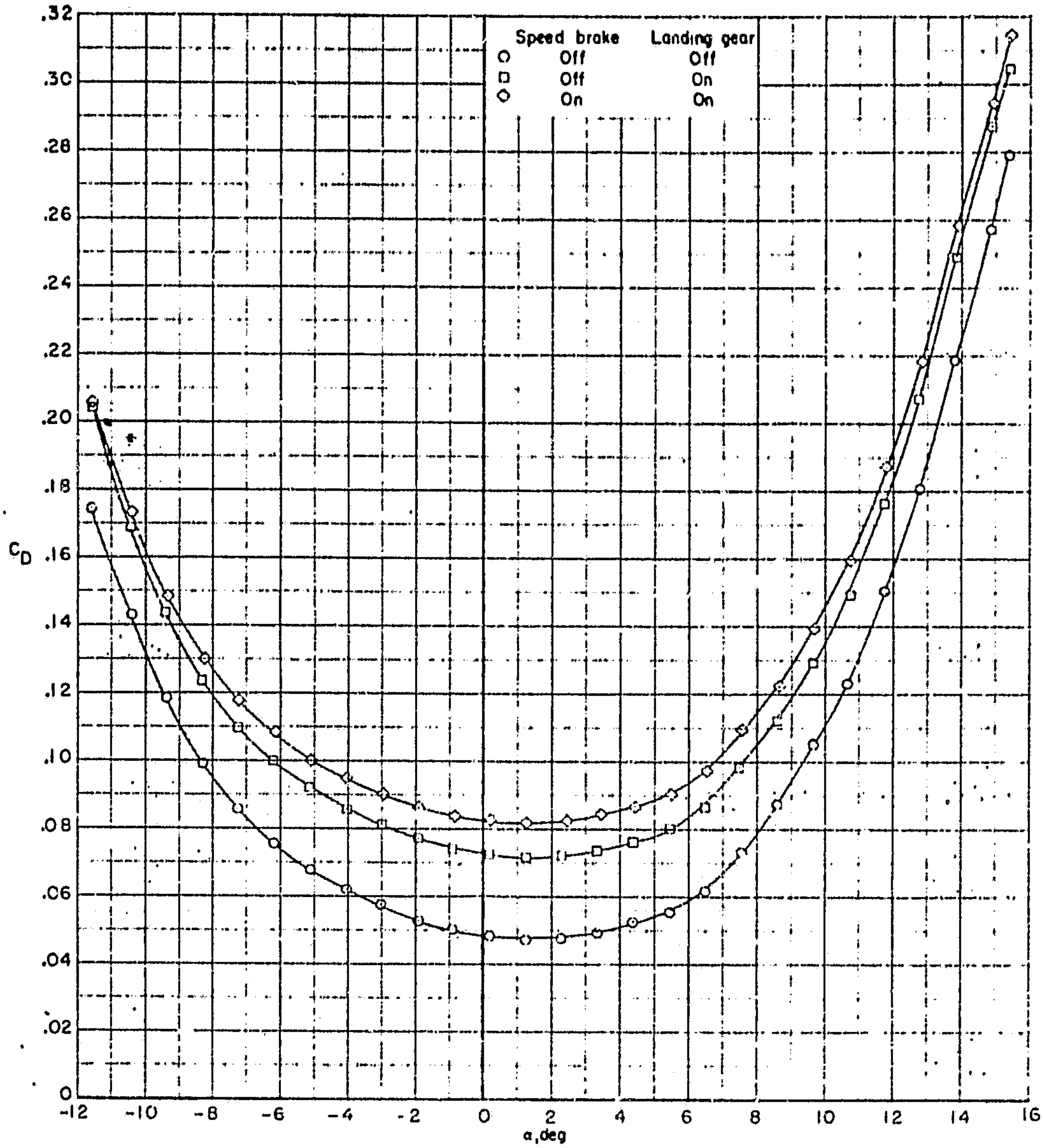

(a) M = 0.25. Continued.

Figure 4.- Continued.

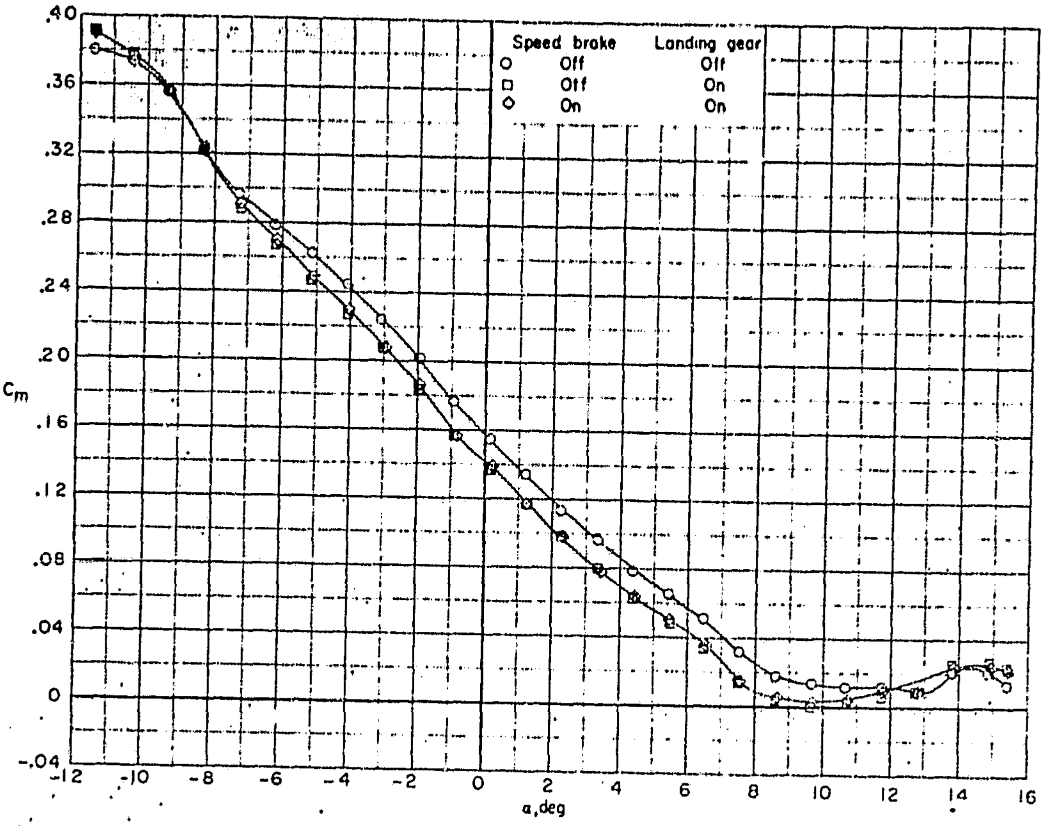

(a) M = 0.25. Concluded.

Figure 4.- Continued.

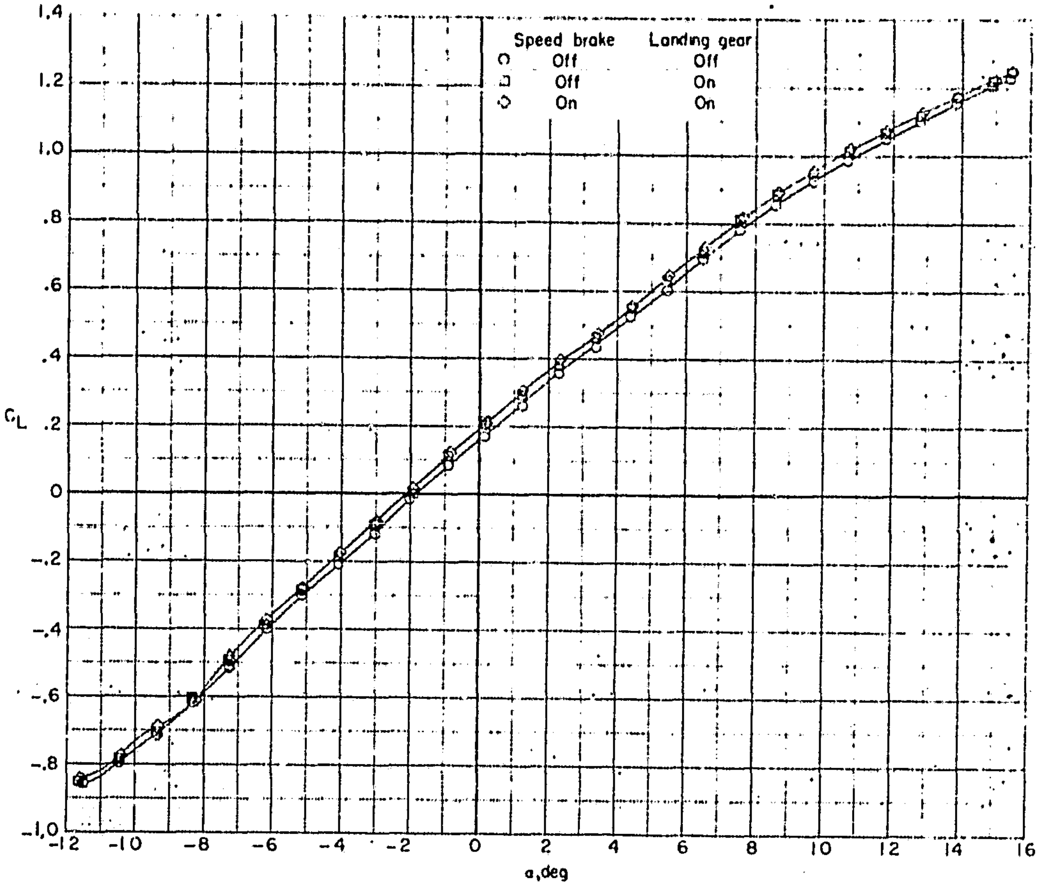

(b) M = 0.35.

Figure 4.- Continued.

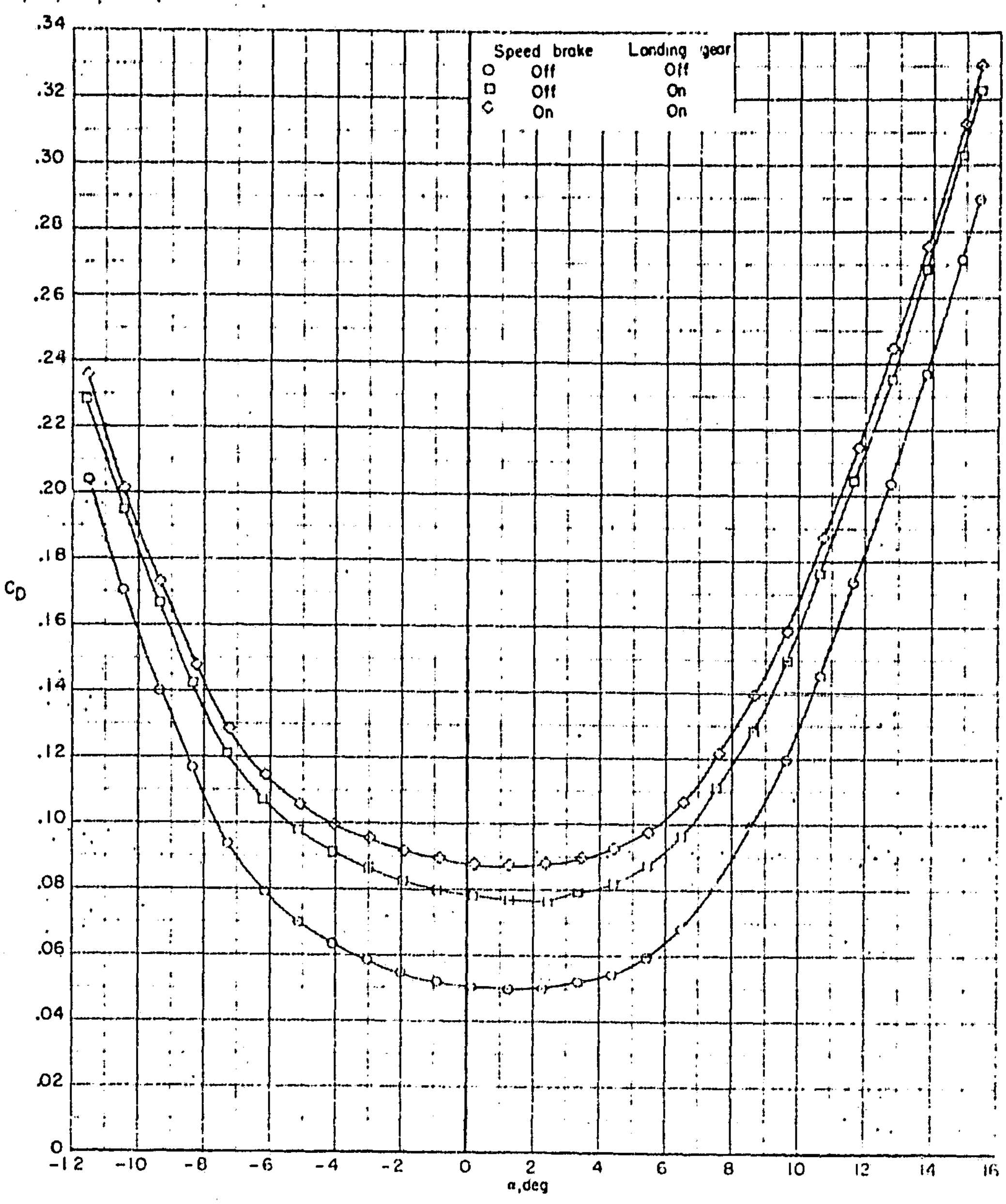

(b) M = 0.35. Continued.

Figure 4.- Continued.

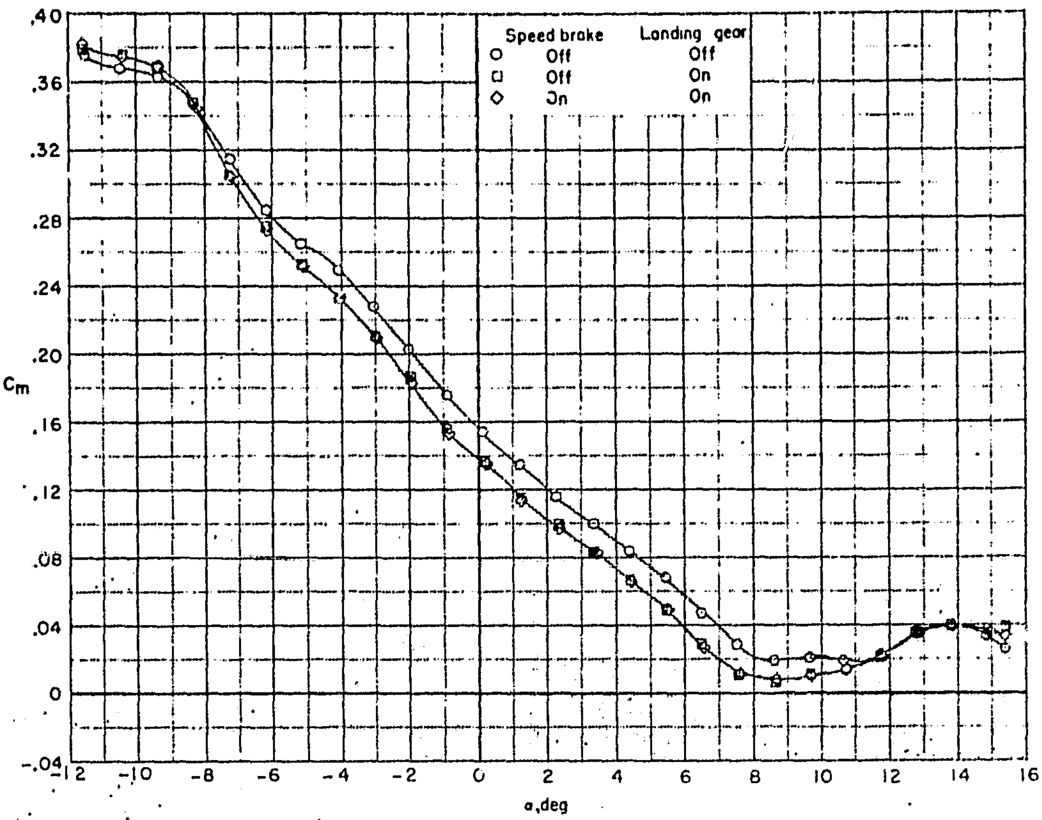

(b) M = 0.35. Concluded.

Figure 4.- Concluded.

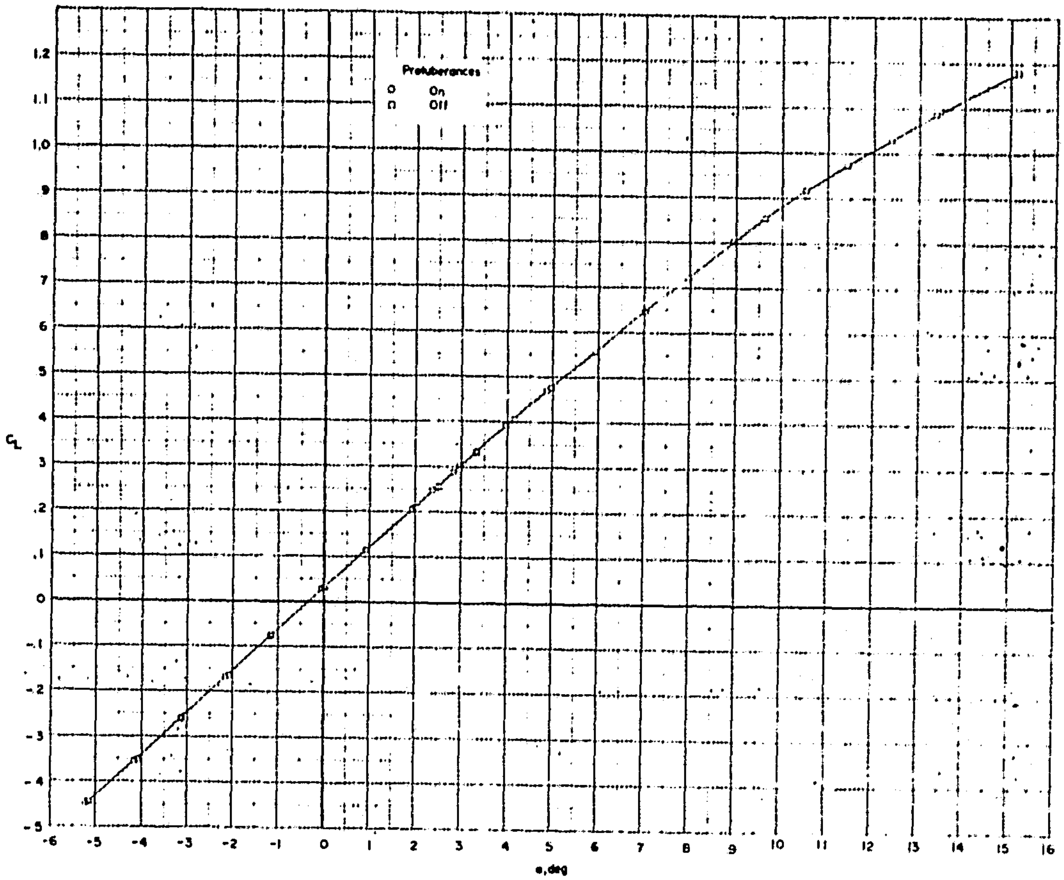

(a) M = 0.50.

Figure 5.- Effect of protuberances on longitudinal aerodynamic characteristics. $\delta_h = -2.5°$; $\delta_f = 0°$.

ORIGINAL PAGE IS
OF POOR QUALITY

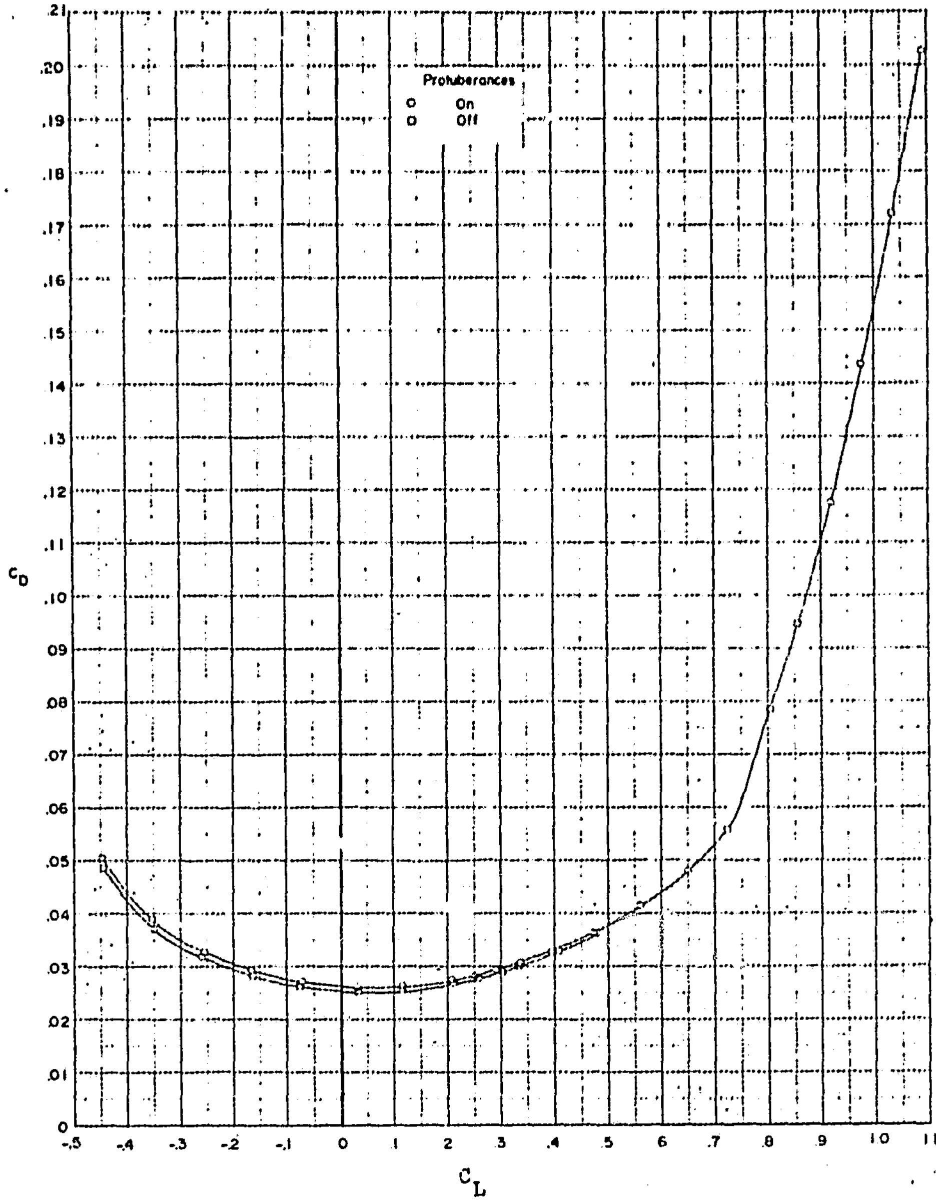

(a) M = 0.50. Continued.

Figure 5.- Continued.

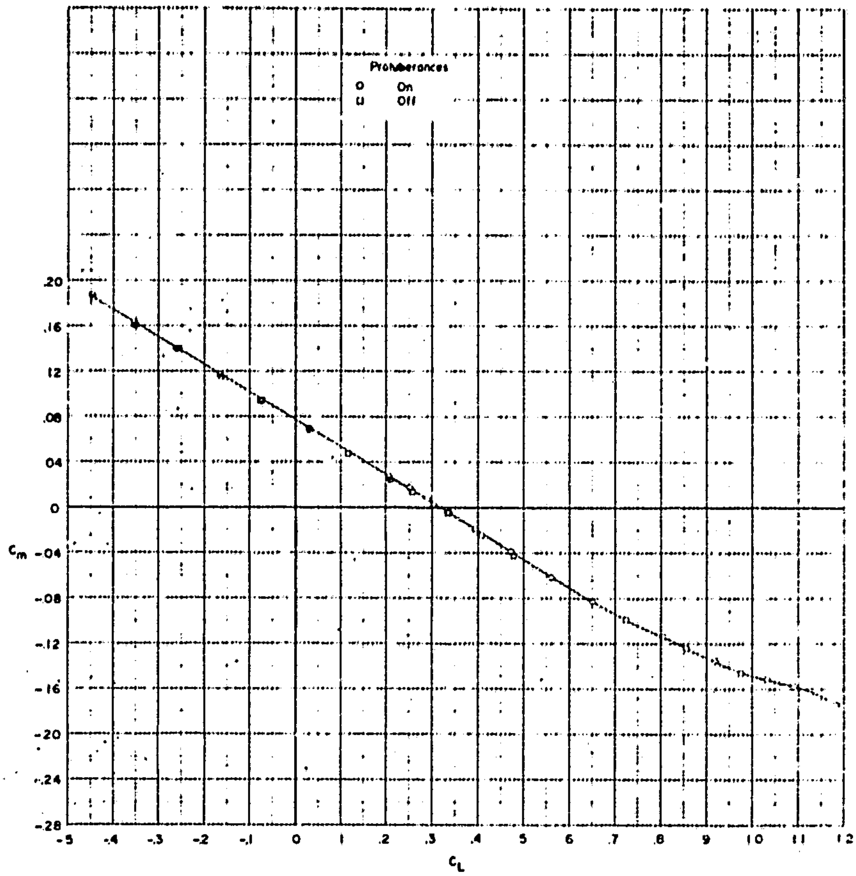

(a) M = 0.50. Concluded.

Figure 5.- Continued.

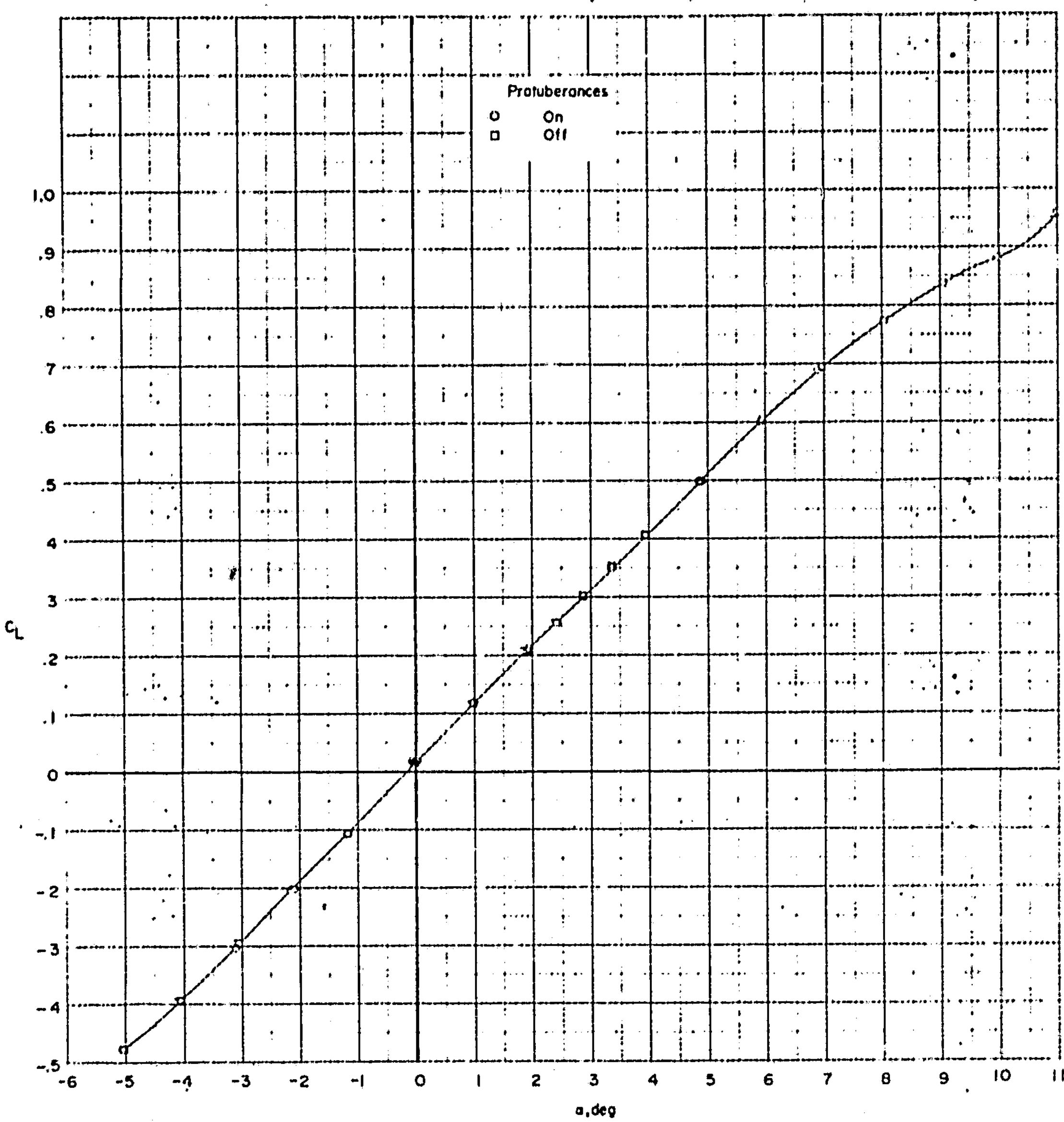

(b) M = 0.80.

Figure 5.- Continued.

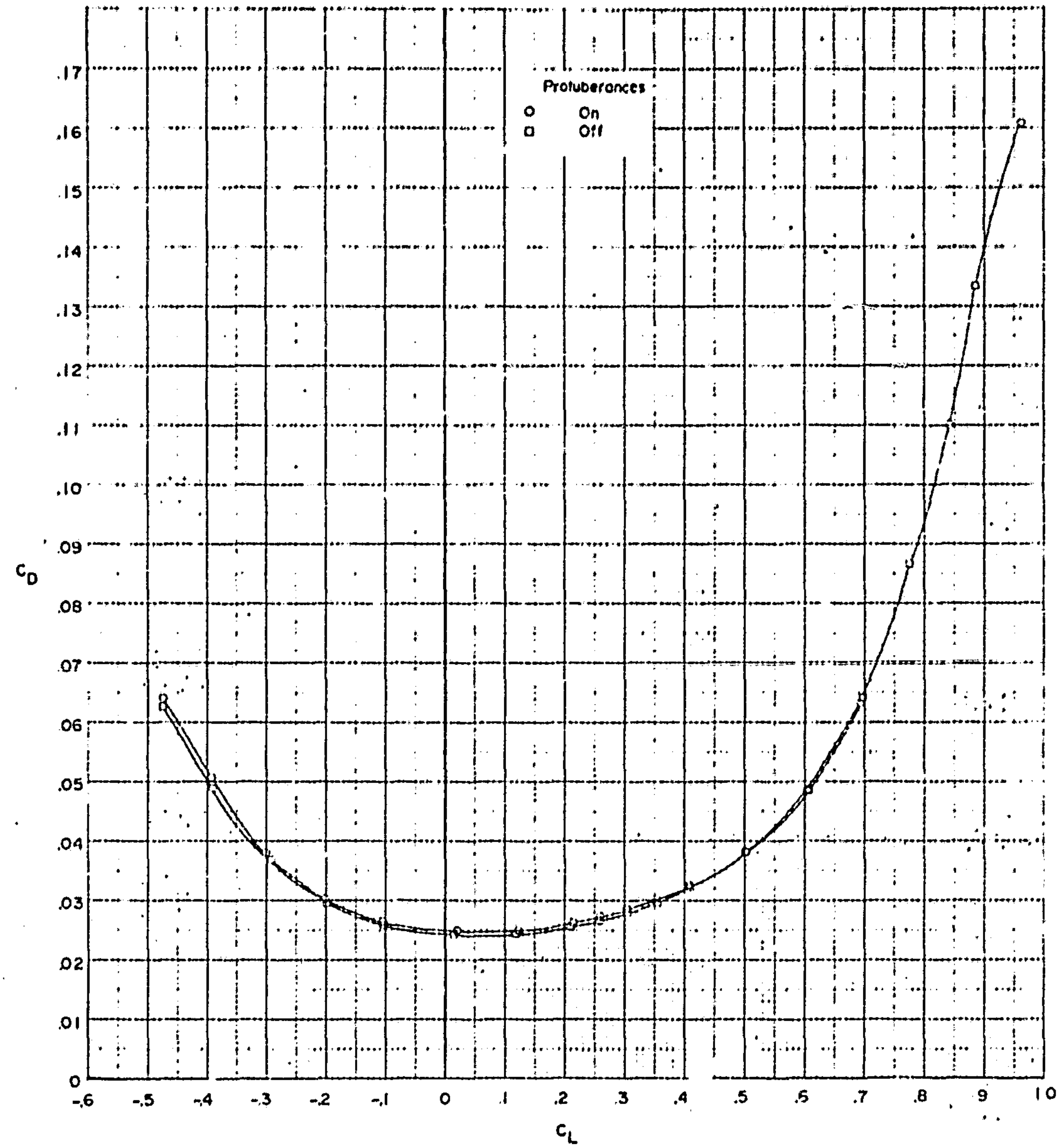

(b) M = 0.80. Continued.

Figure 5.- Continued.

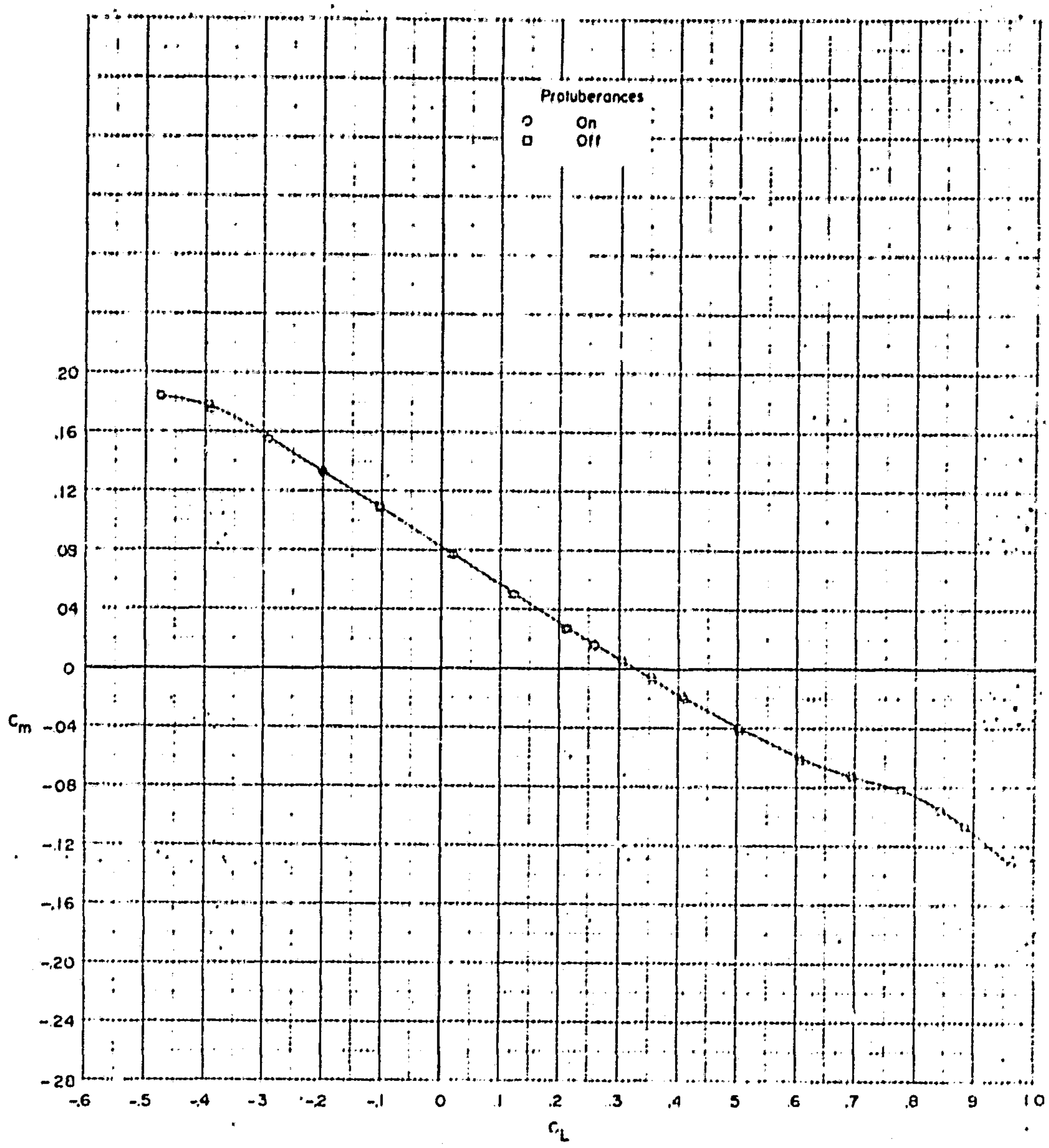

(b) M = 0.80. Concluded.

Figure 5.- Continued.

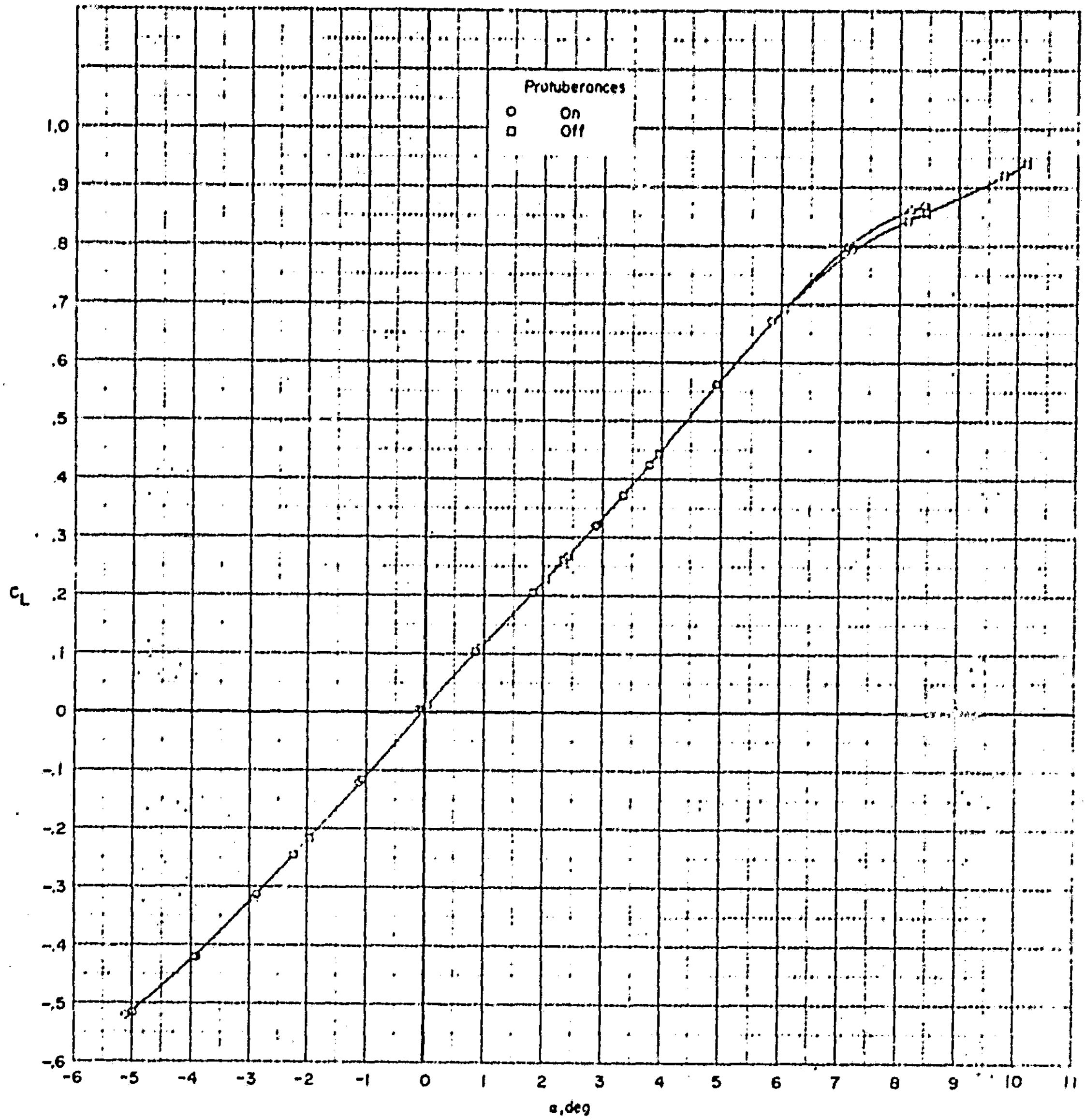

(c) M = 0.90.

Figure 5.- Continued.

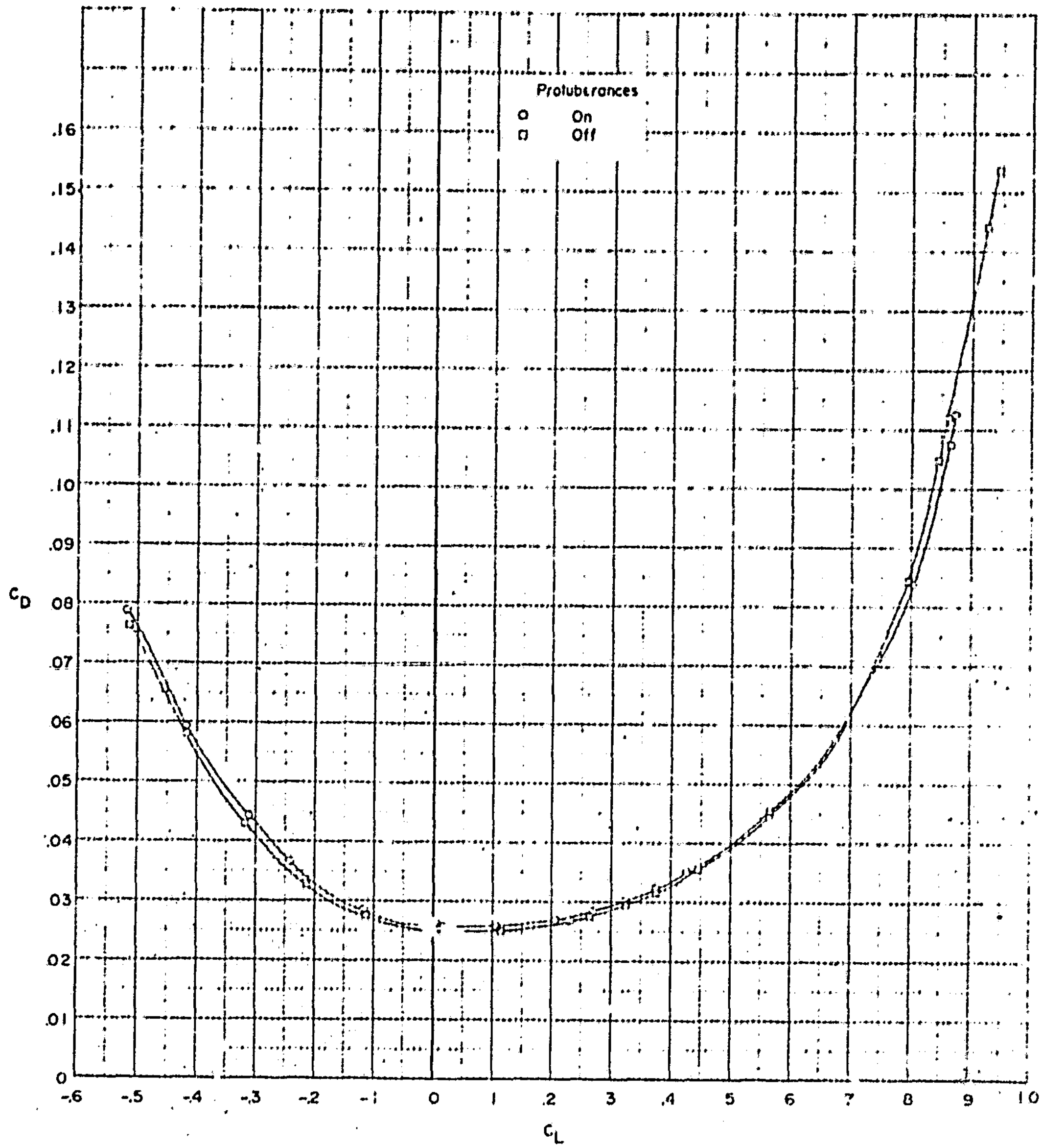

(c) M = 0.90. Continued.

Figure 5.- Continued.

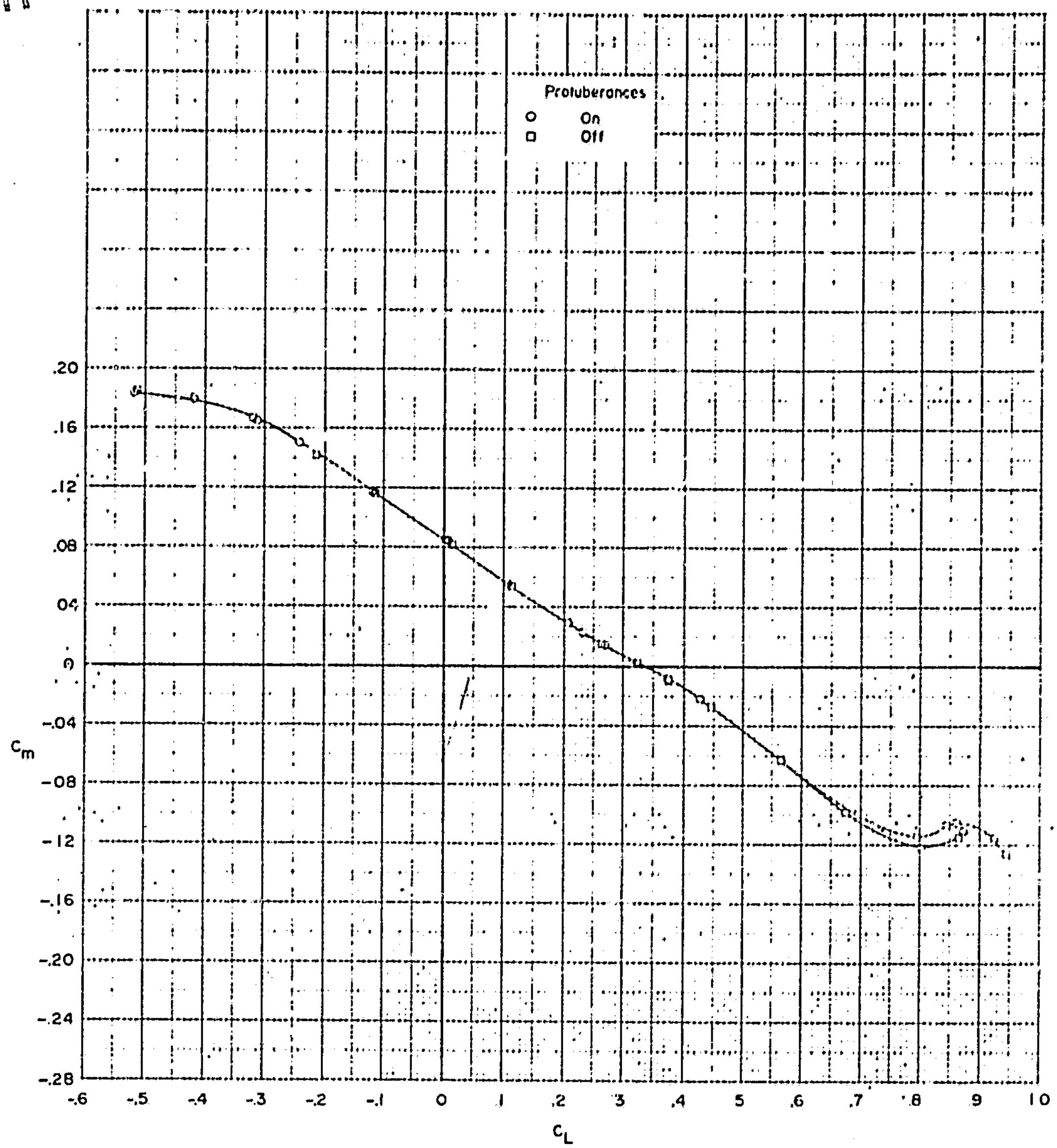

(c) M = 0.90. Concluded.

Figure 5.- Continued.

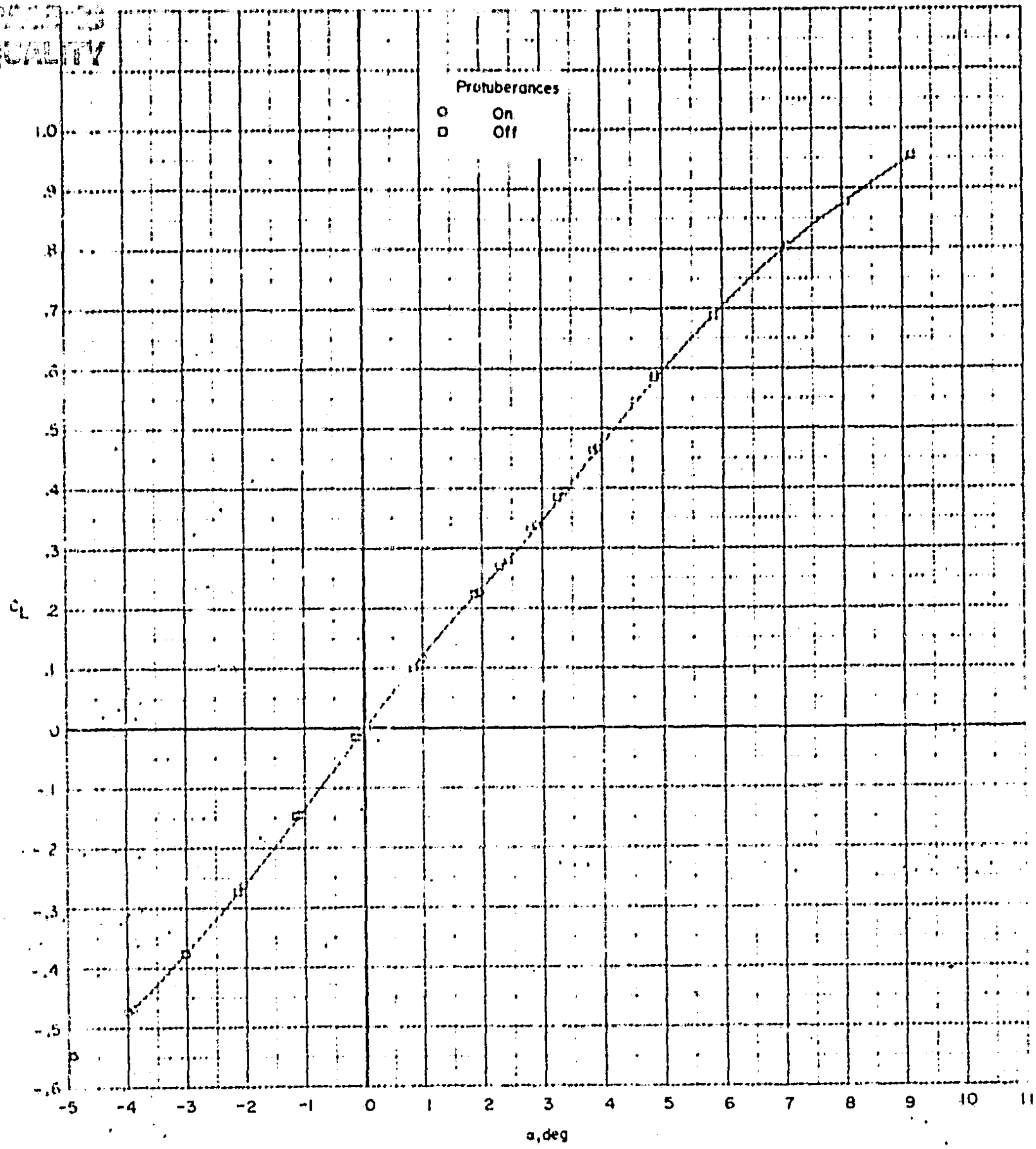

(d) M = 0.95.

Figure 5.- Continued.

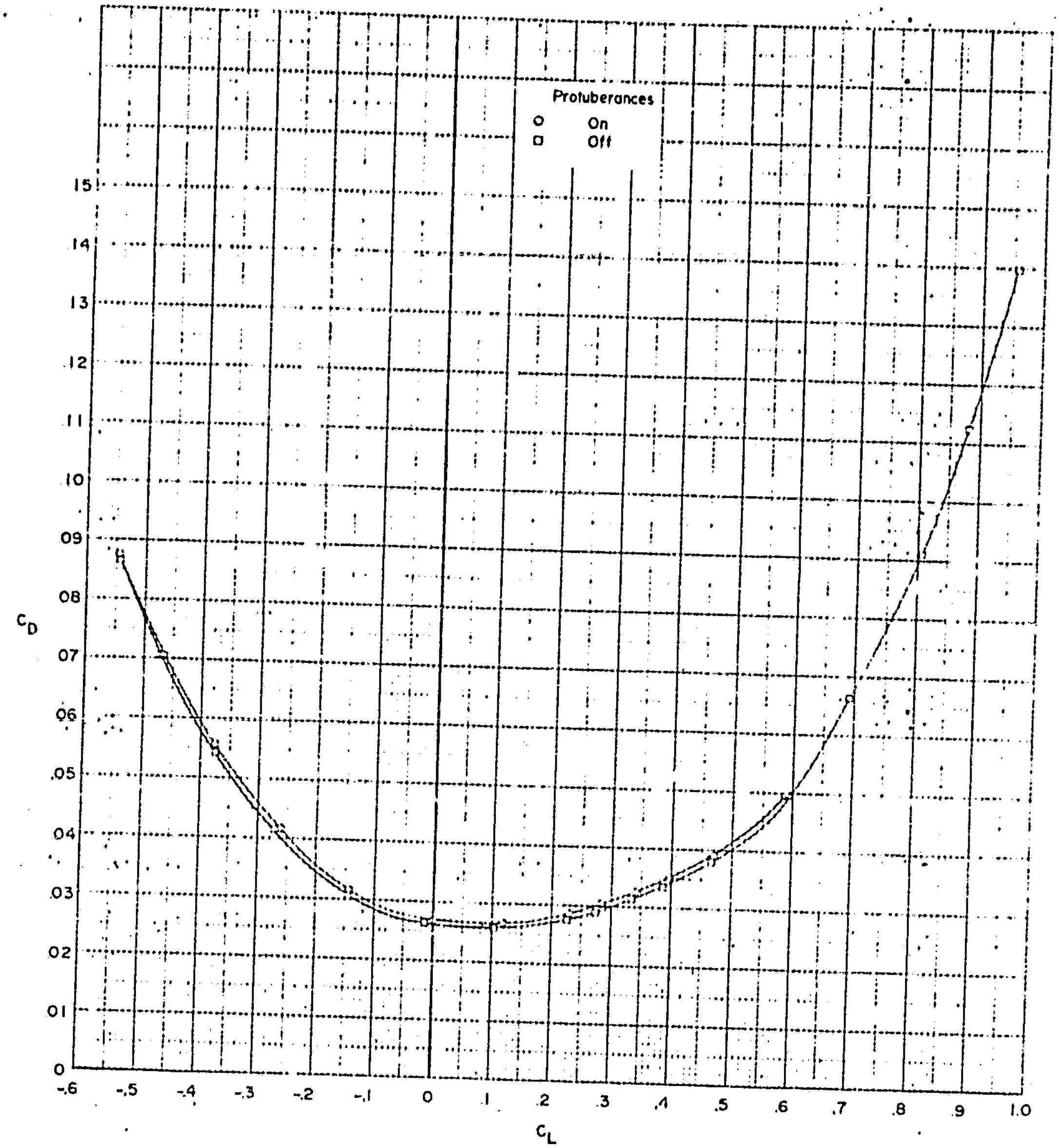

(d) M = 0.95. Continued.

Figure 5.- Continued.

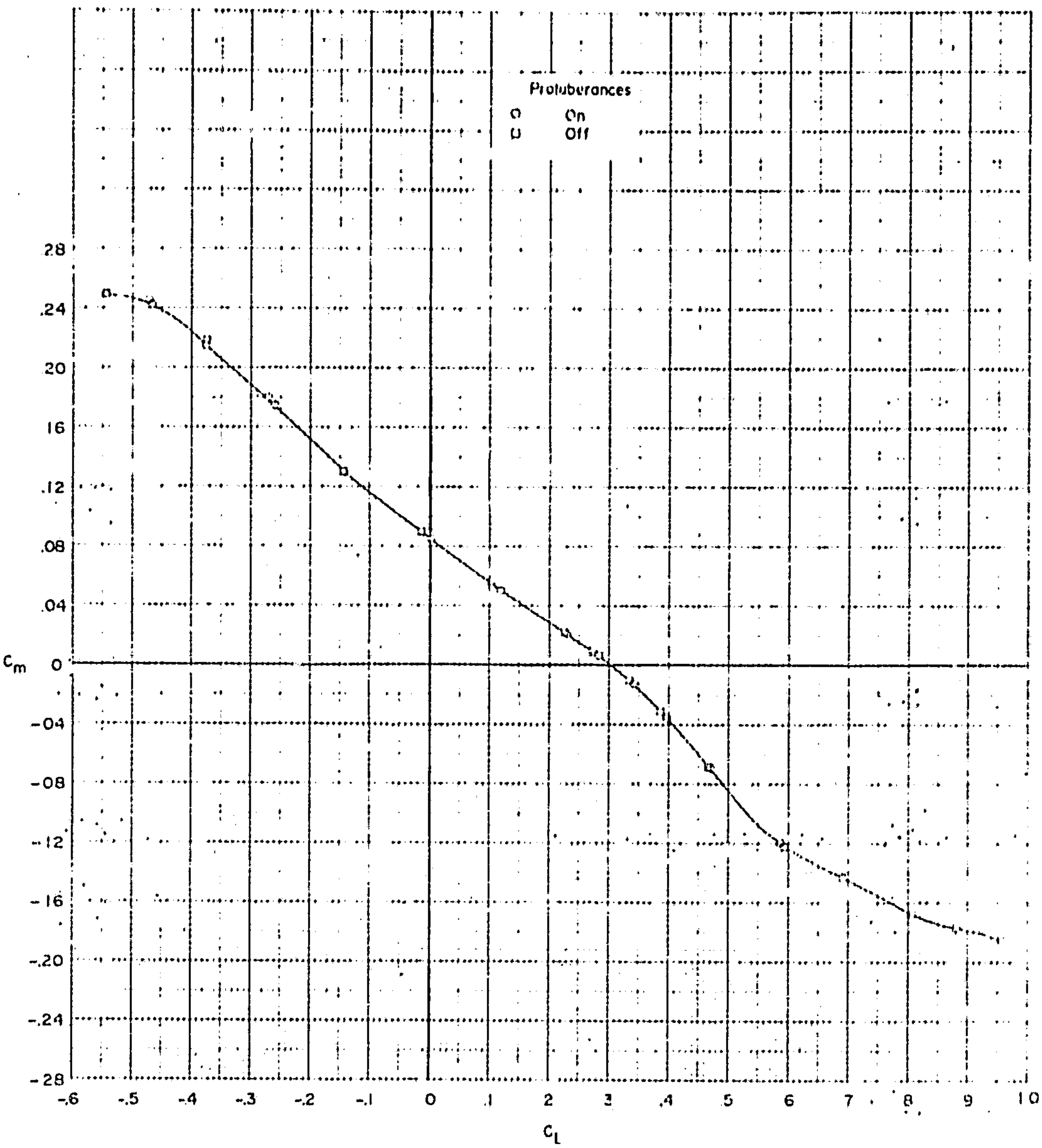

(d) M = 0.95. Concluded.

Figure 5.- Continued.

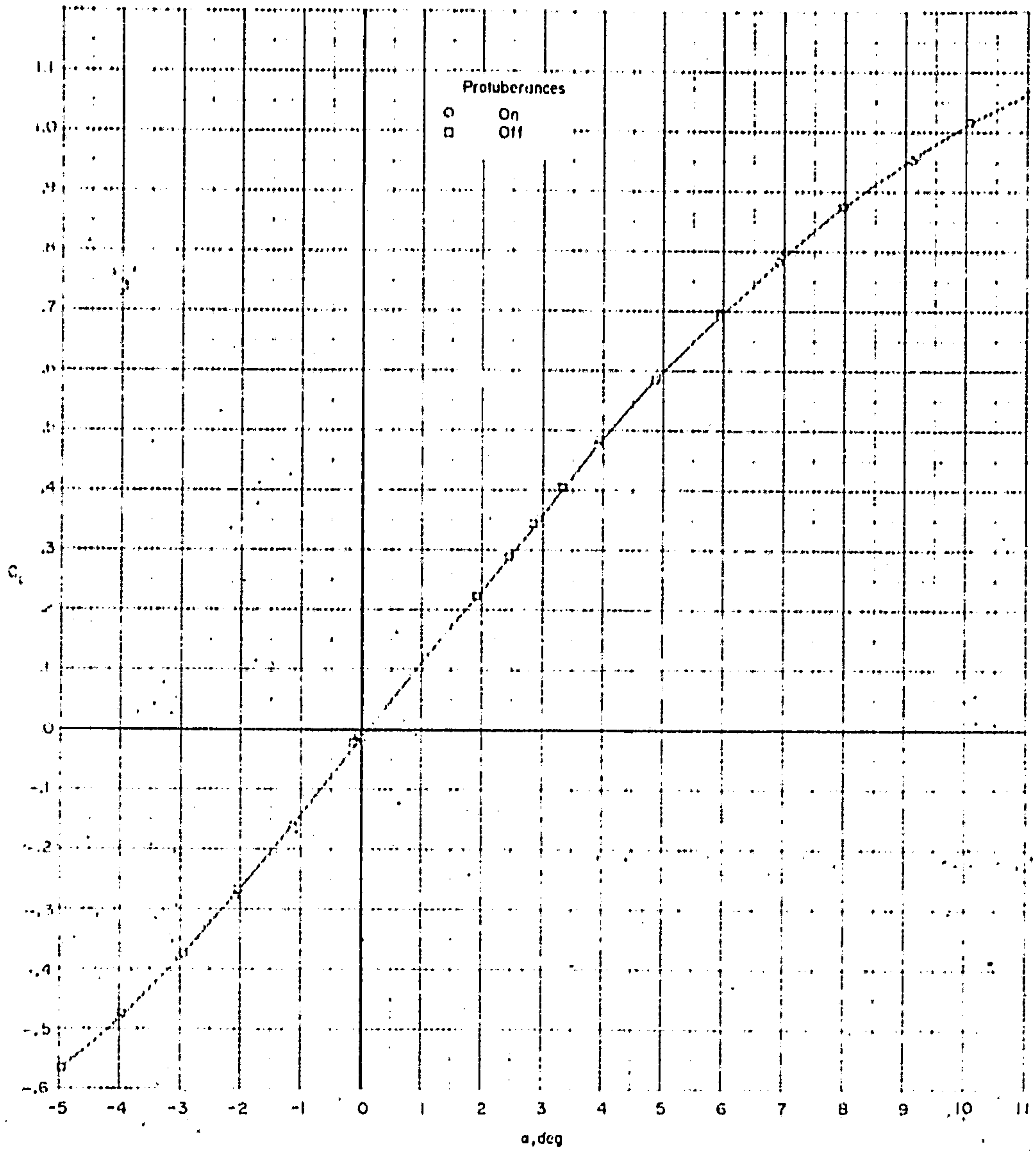

(e) M = 0.97.

Figure 5. - Continued.

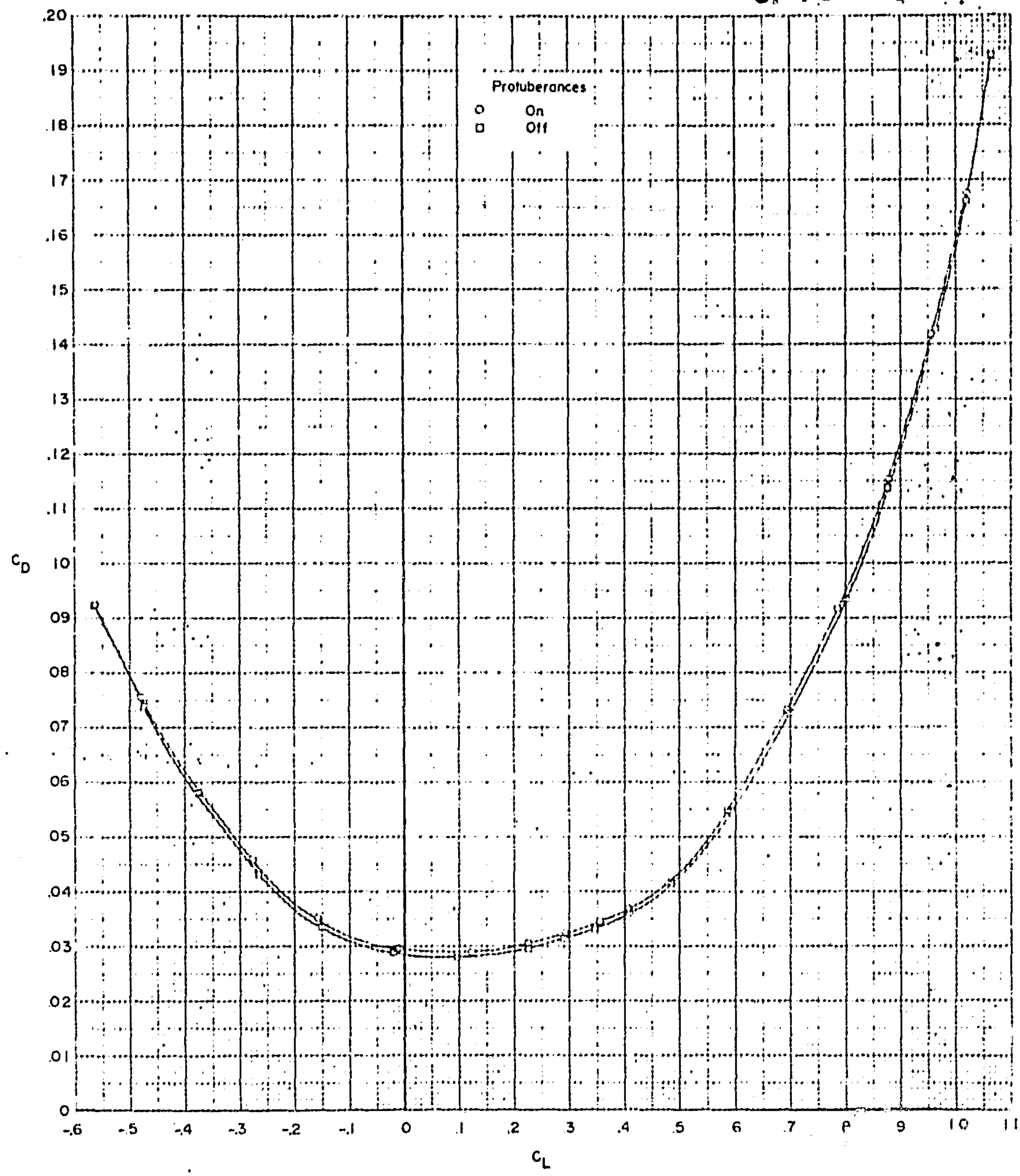

(e) M = 0.97. Continued.

Figure 5.- Continued.

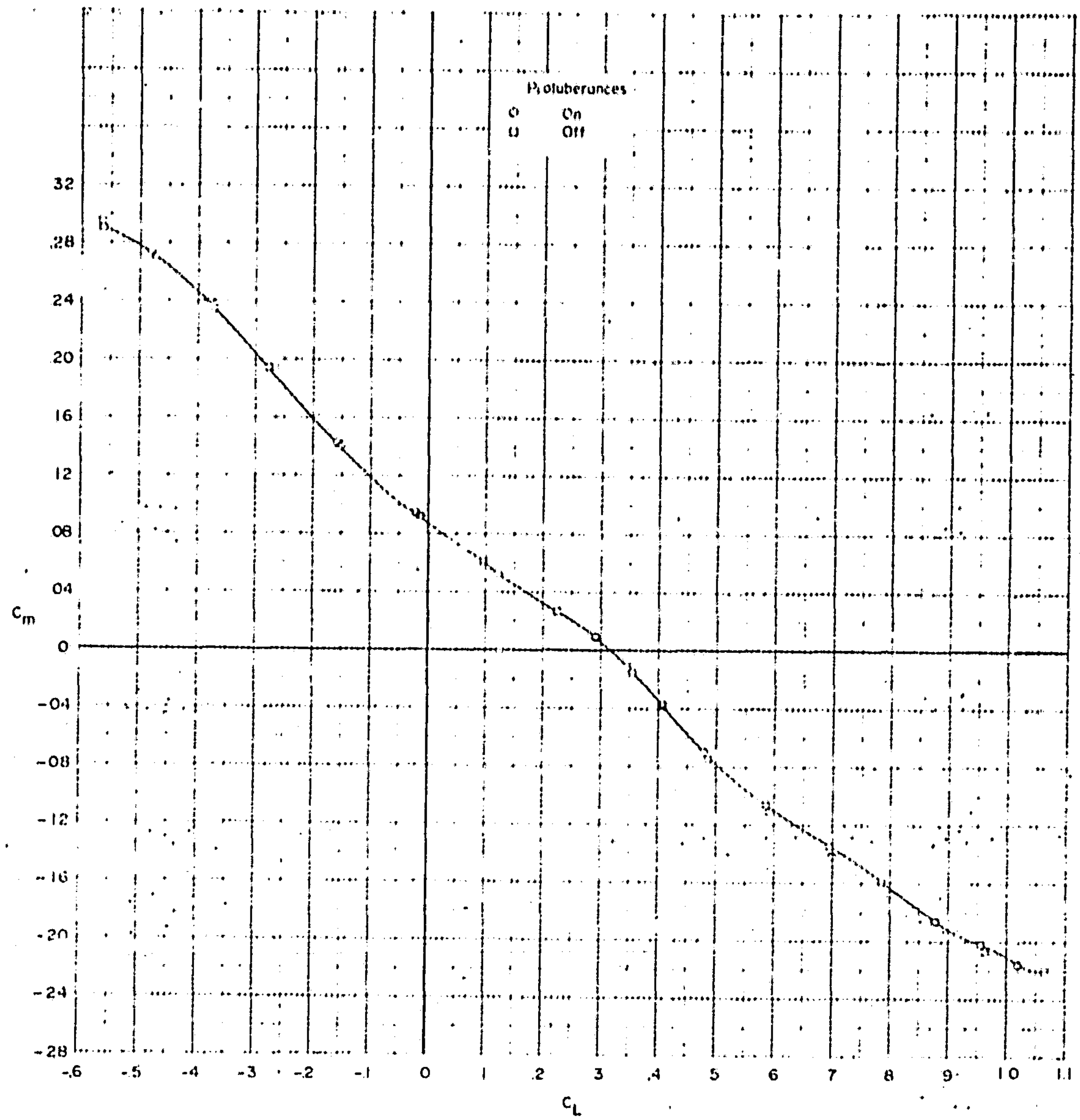

(e) M = 0.97. Concluded.

Figure 5.- Continued.

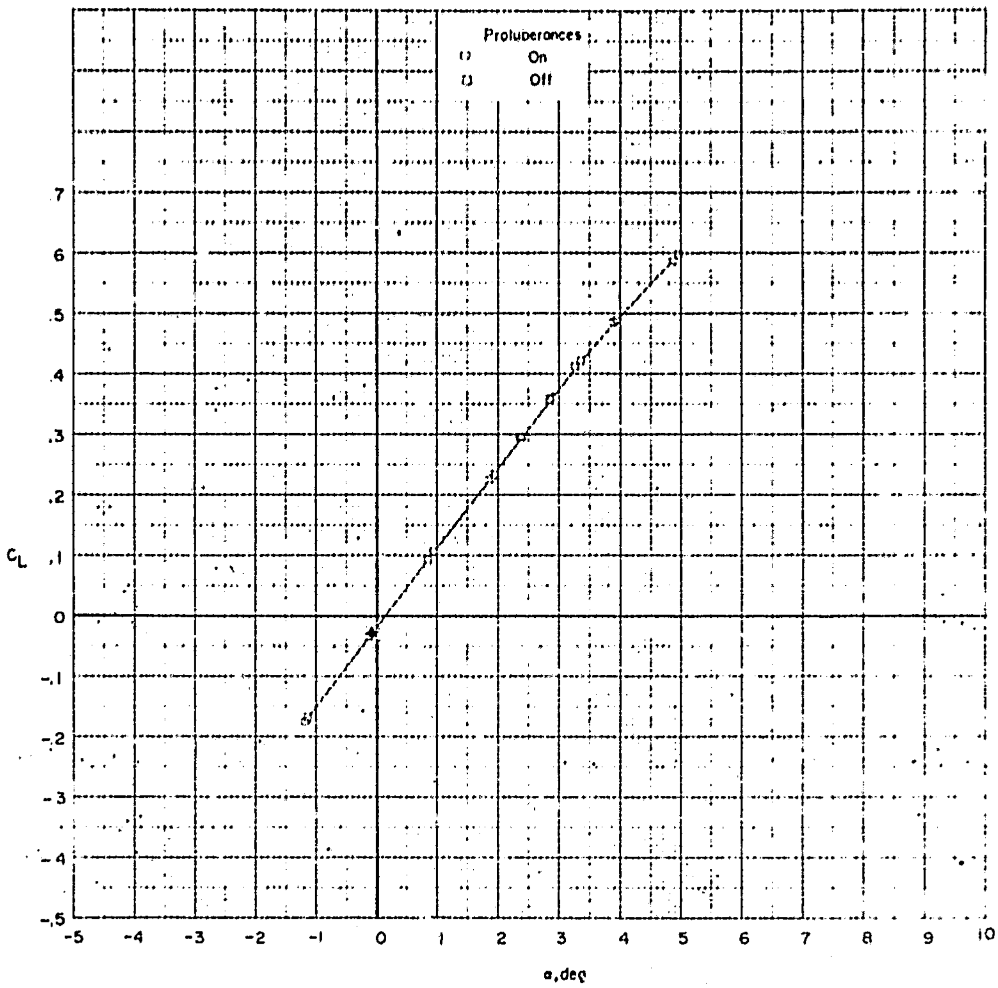

(f) M = 0.98.

Figure 5.- Continued.

ORIGINAL PAGE IS
OF POOR QUALITY

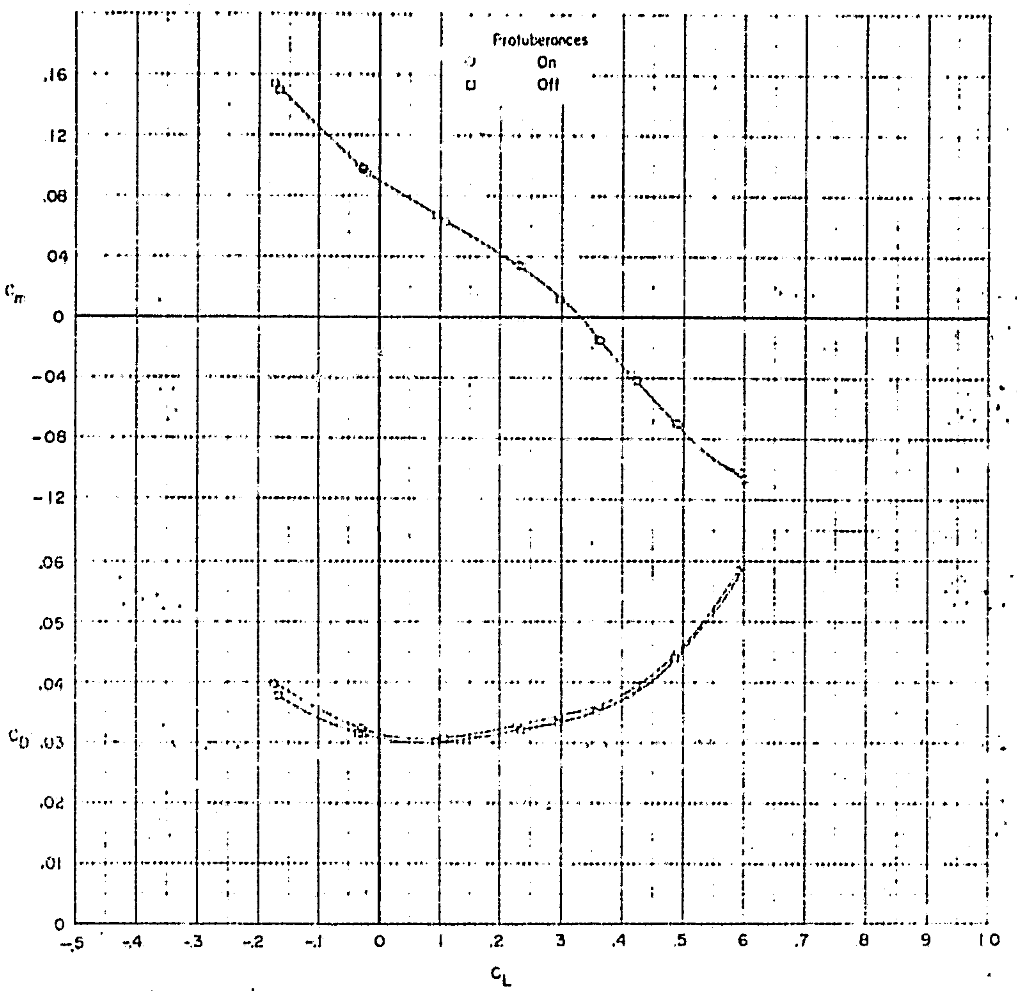

(f) M = 0.98. Concluded.

Figure 5.- Continued.

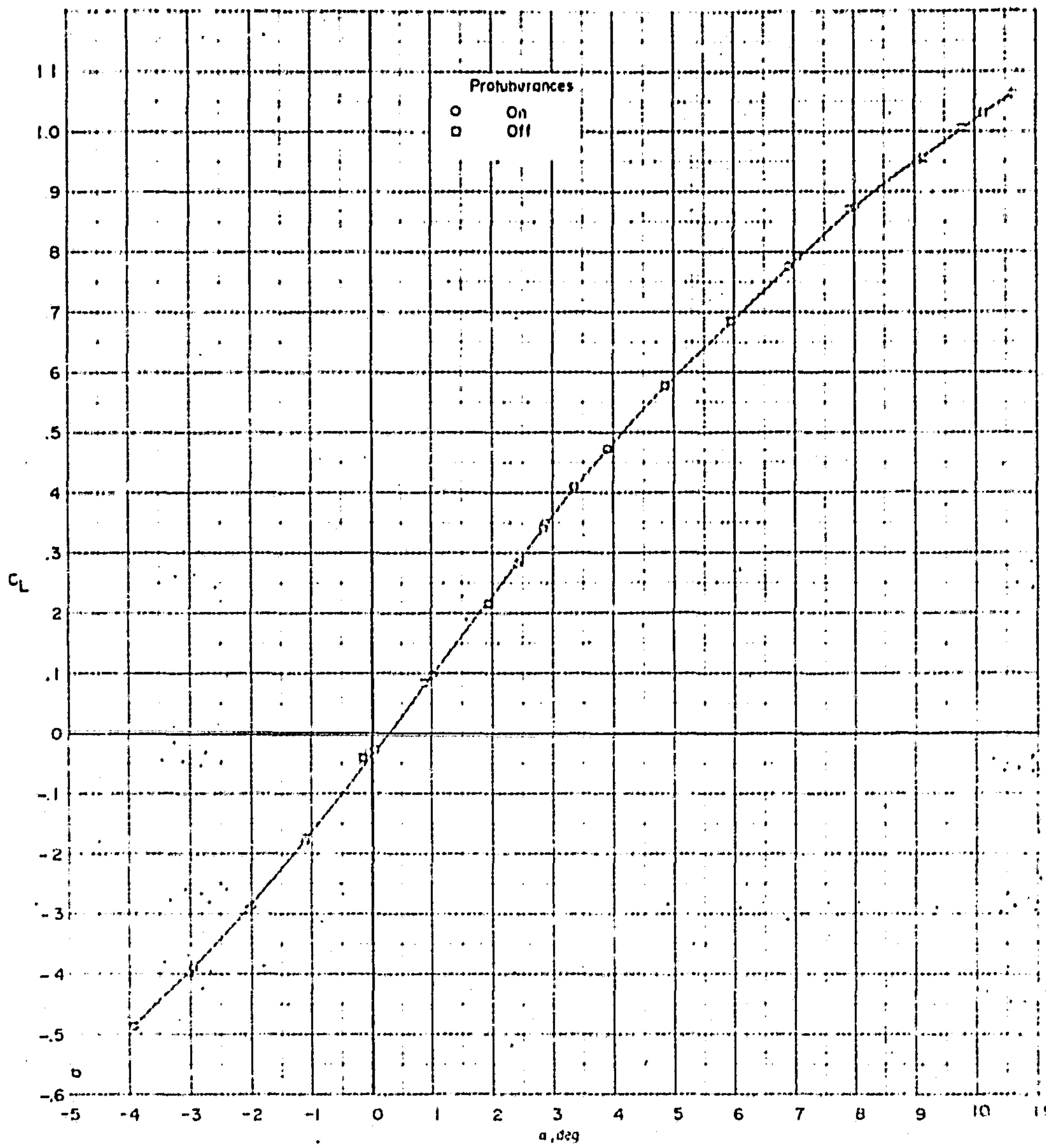

(g) M = 0.99.

Figure 5.- Continued.

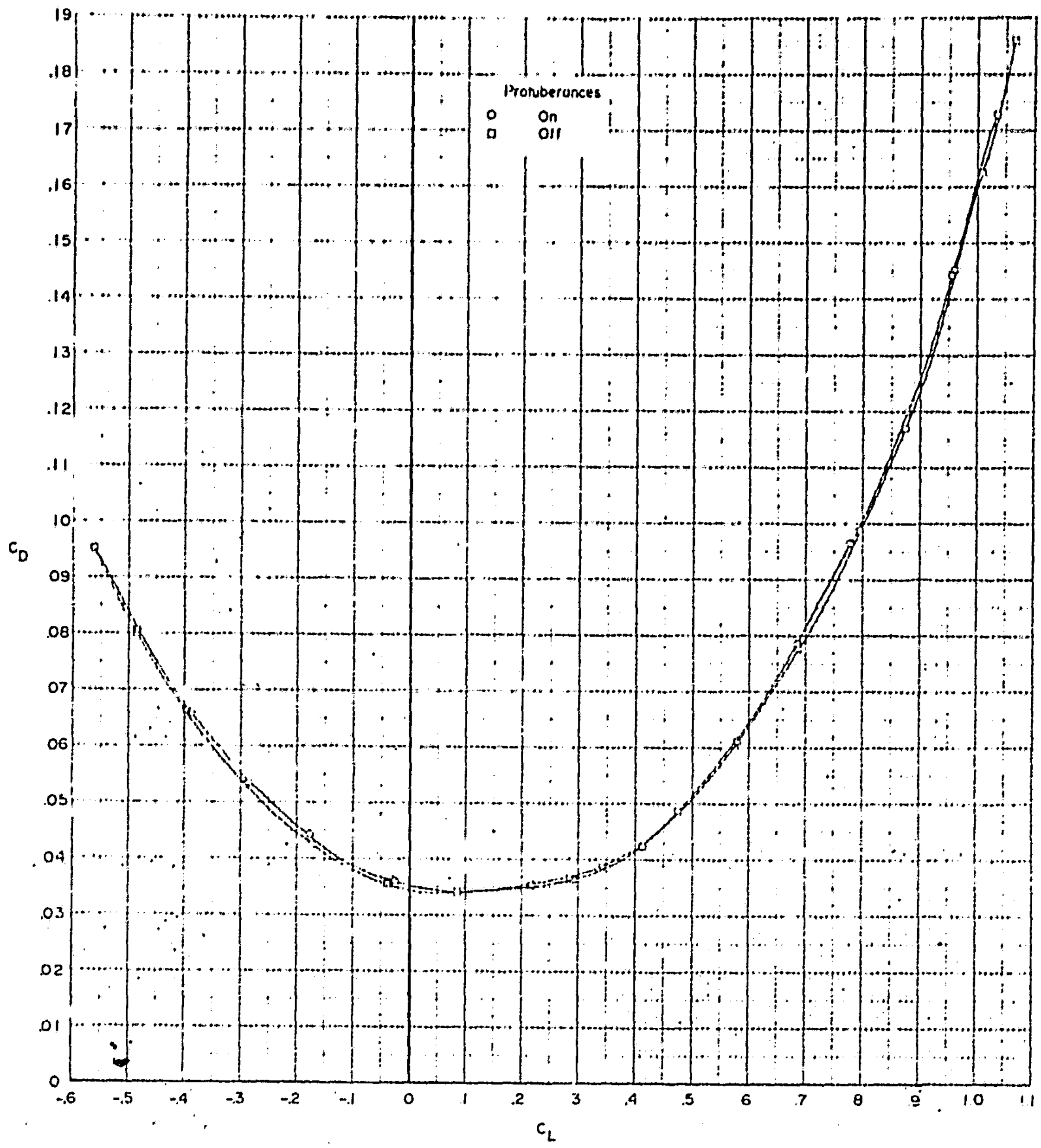

(g) M = 0.99. Continued.

Figure 5.- Continued.

ORIGINAL PAGE IS
OF POOR QUALITY

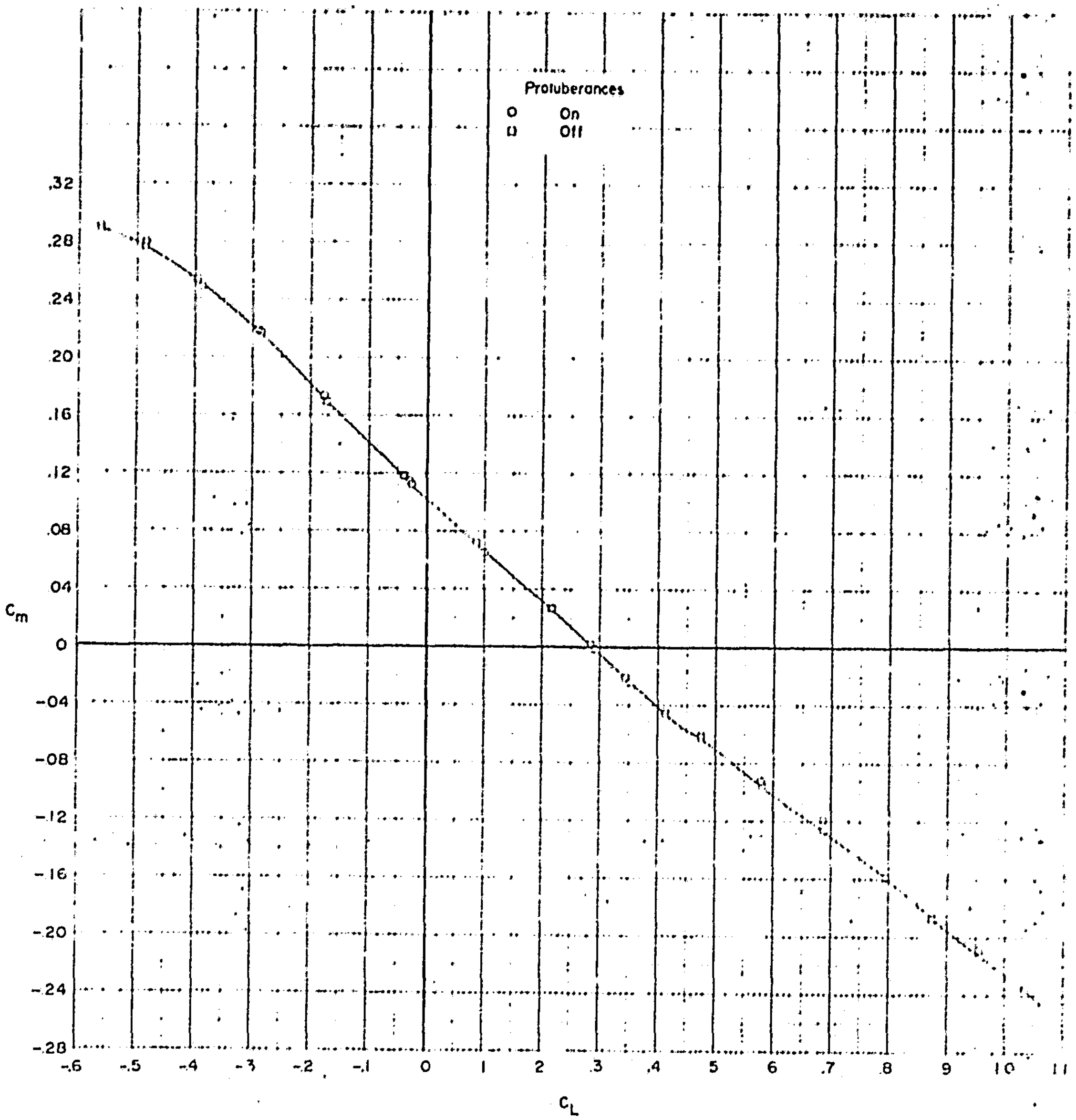

(g) M = 0.99. Concluded.

Figure 5.- Continued.

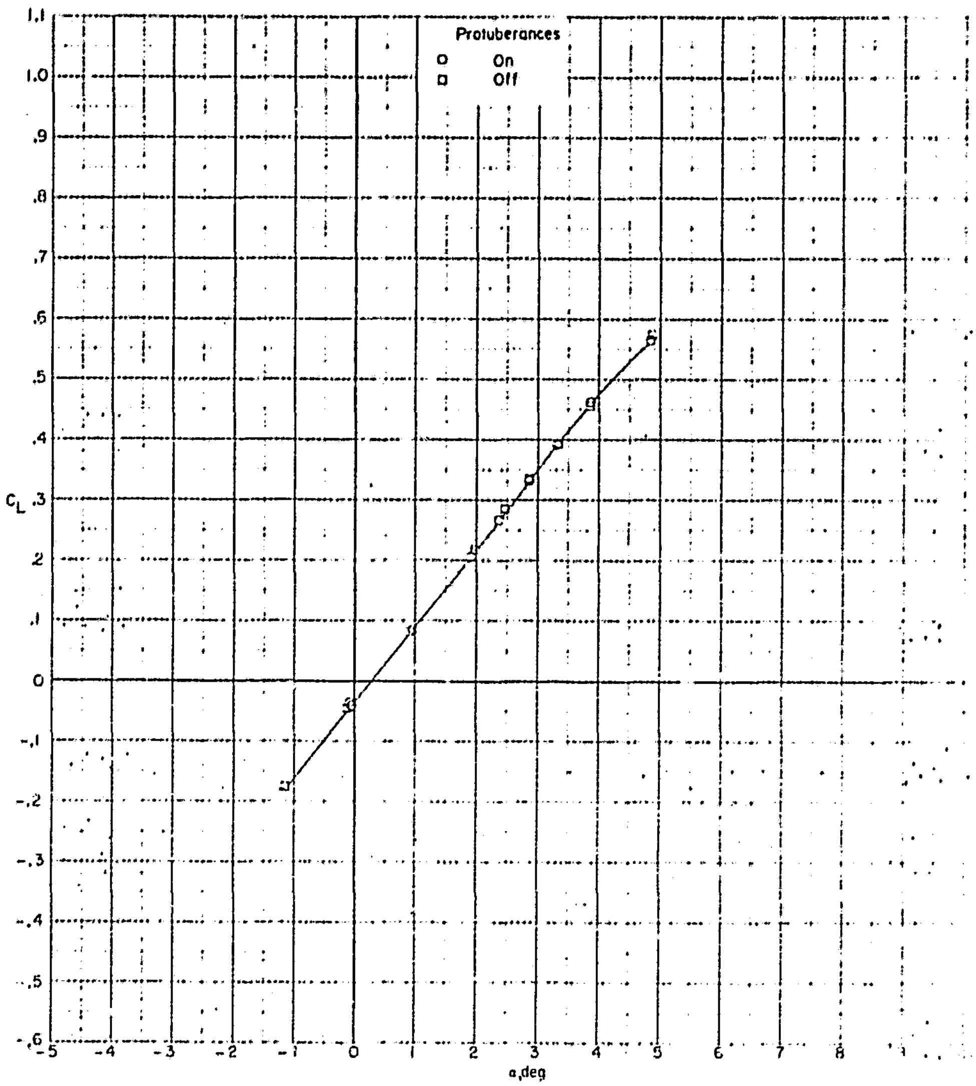

(h) M = 1.00.

Figure 5.- Continued.

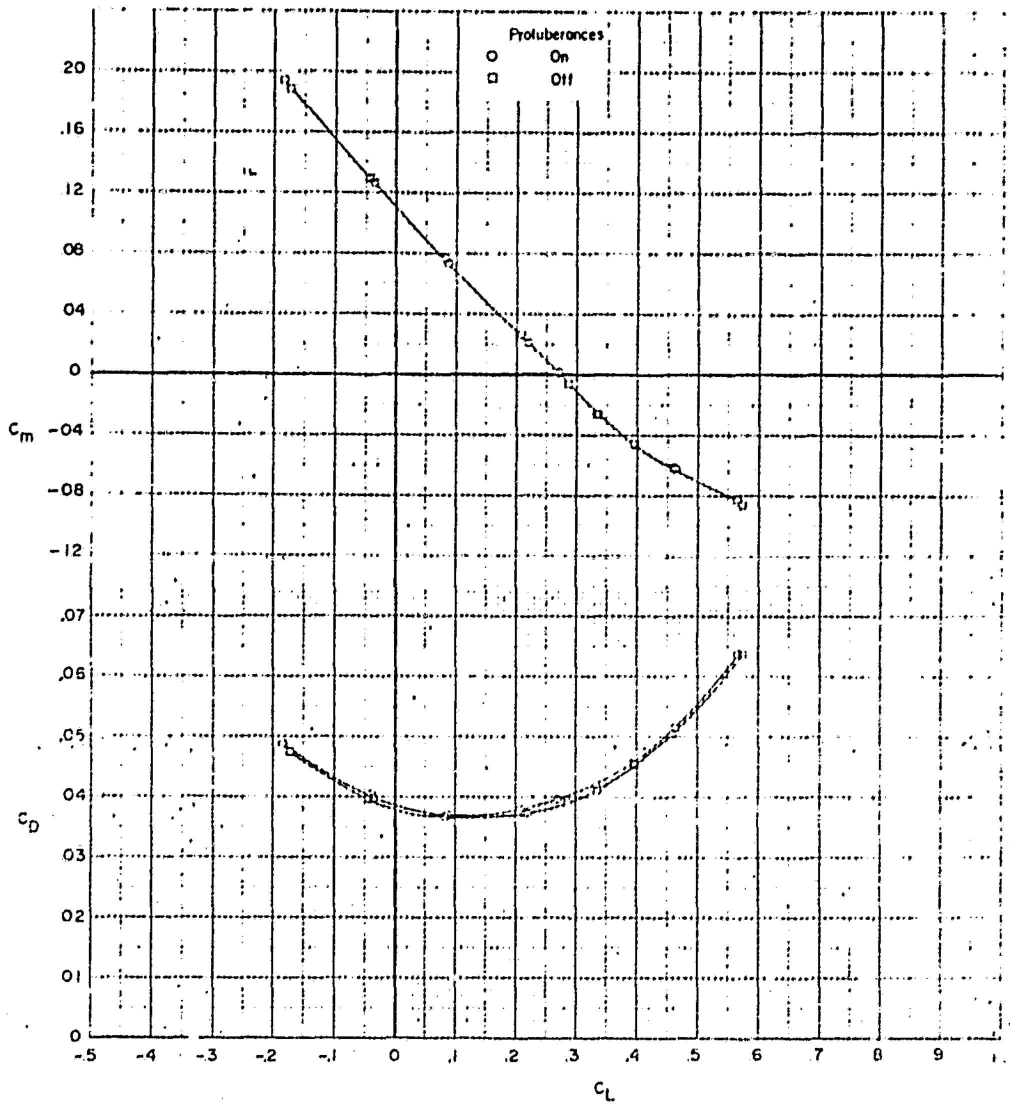

(h) M = 1.00. Concluded.

Figure 5.- Concluded.

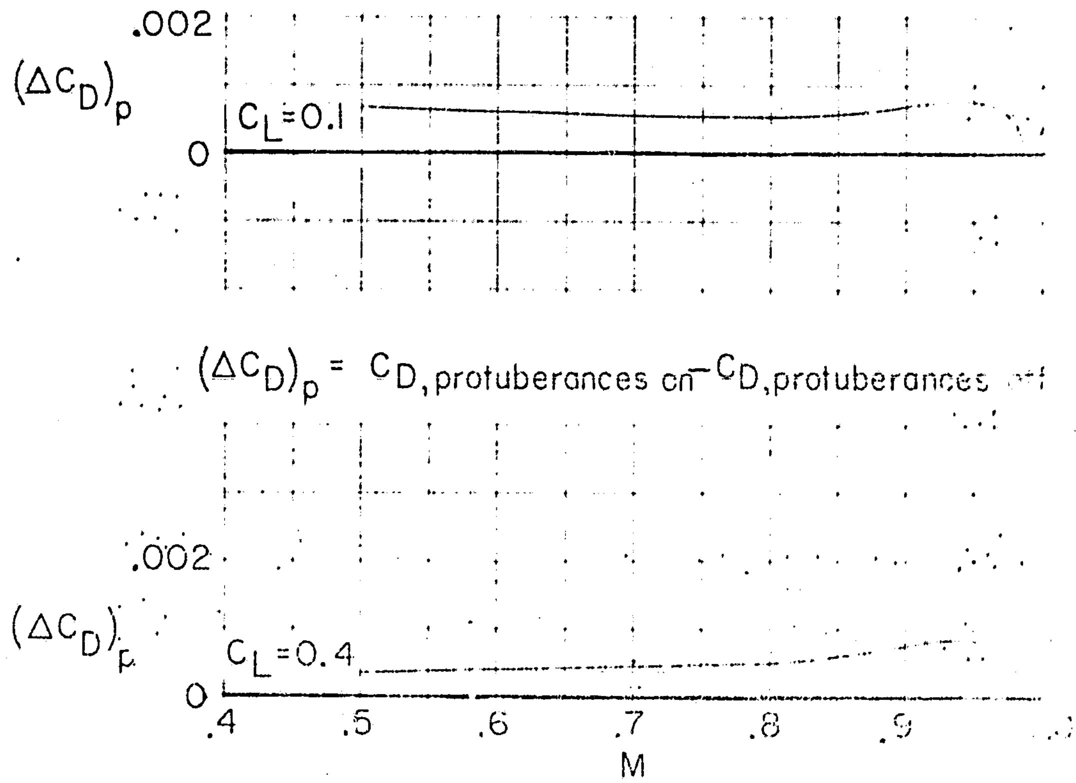

Figure 6.- Variation with Mach number of the drag increment due to protuberances.